

1 **Title**

2 Phosphorus mineral evolution and prebiotic chemistry: from minerals to
3 microbes

4 **Authors**

5 Craig R. Walton^{1*}, Oliver Shorttle^{1,2}, Frances E. Jenner³, Helen M. Williams¹, Joshua
6 Golden⁴, Shaunna M. Morrison⁴, Robert T. Downs⁴, Aubrey Zerkle⁵, Robert M. Hazen⁶,
7 Matthew Pasek⁷

8
9 **Affiliations**

10 ¹ Department of Earth Sciences, University of Cambridge, Downing Street,
11 Cambridge CB2 3EQ, UK

12 ² Institute of Astronomy, University of Cambridge, Madingley Road, Cambridge,
13 CB3 0HA, UK

14 ³ School of Environment, Earth and Ecosystem Sciences, The Open University,
15 Walton Hall, Milton Keynes MK7 6AA, UK

16 ⁴ Department of Geosciences, University of Arizona, 1040 E. 4th Street, Tucson,
17 AZ 85721, USA

18 ⁵ School of Earth and Environmental Sciences, University of St Andrews, Irvine
19 Building, KY16 9AL

20 ⁶ Geophysical Laboratory, Carnegie Institution for Science, 5251 Broad Branch
21 Road, NW, Washington, DC 20015, UK

22 ⁷ School of Geoscience, University of South Florida, 4202 E Fowler Ave, Tampa
23 FL 33620, USA

24 *crw59@cam.ac.uk

25 **Abstract**

26

27 Phosphorus availability is considered a limiting factor in many scenarios for the origin of life. The
28 concentration of P in environments of prebiotic interest will have been governed by the available
29 mineral sources of P on the early Earth. A knowledge of early Earth P mineralogy and prevailing
30 global and local environmental conditions is therefore needed to understand which scenarios for
31 prebiotic chemistry are most plausible. Here, we review the plausible diversity of P-bearing
32 phases at Earth's surface during the emergence of life. We consider phases that were delivered by
33 meteorites (exogenous phases), as well as those that developed solely as a result of Earth system
34 processes (endogenous phases). We take into account the known formation conditions of
35 individual phases, as well as the observed temporal distributions of P-bearing minerals found at
36 Earth's surface today. Our approach allows us to leverage what is known about changes in the
37 Earth system in order to rule out the prebiotic relevance of many P-bearing phases. Meanwhile,
38 we highlight a small number of phases that are of possible prebiotic relevance; specifically,
39 exogenous schreibersite, merrillite, and apatite, and endogenous apatite, olivine, and glass.
40 Prebiotic mineral-chemical scenarios can be formulated for each phase, with distinct requirements
41 for the environmental and tectonic state of early Earth. We can therefore relate the plausibility of
42 mineral-chemical scenarios to the nature of early Earth, bridging the fields of geoscience and
43 prebiotic chemistry.

44

45

46

47

48

49

50

51 **Introduction**

52 Minerals are known to control the availability of non-volatile and bio-essential elements at
53 Earth's surface. Therefore, the role of minerals in prebiotic chemistry is a focal point of research
54 into the origins of life. However, the mineralogical diversity of earliest Earth is not definitively
55 known. This uncertainty is owed both to progressive change in the Earth system, which makes the
56 present an imperfect guide to the past, and a progressively incomplete rock record of Earth history
57 with increasing age. Hence, much is unknown about the planetary conditions under which
58 terrestrial life first developed, for example the diversity of nutrient-bearing minerals (e.g.,
59 phosphorus – P) in Earth's early crust and surface environments. Here, we review the plausible
60 diversity of P-bearing phases at Earth's surface during the emergence of life.

61

62 All organisms require the element P (atomic number 15) at a fundamental level in order to
63 metabolise (adenosine triphosphate is the 'energy currency of life'), compartmentalise
64 (phospholipids build cell walls), and replicate (phosphate-diester linkages are the backbone of
65 DNA; (Bowler et al., 2010; Fernández-García et al., 2017; Kamerlin et al., 2013; Westheimer,
66 1987). However, just as P is key for extant forms of life, the importance of this element for the
67 chemistry of life's origins is also clear. High P concentrations (typically as the oxidised species
68 PO_4^{3-}) are a vital constituent of many recent prebiotic reaction schemes (Islam and Powner, 2017;
69 Liu et al., 2019; Pasek et al., 2017; Patel et al., 2015), allowing for efficient pH buffering to
70 ensure clean reaction steps. Phosphorus is required in abundance to drive efficient pre-enzymatic
71 phosphorylation of organic compounds, without which it is challenging to access universal
72 components of known biology e.g., nucleic acid.

73

74 Phosphorus can exist in the following principal redox states: P^{3-} , P^0 , P^{1+} , P^{3+} , and P^{5+} (Pasek et al.,
75 2017). The geochemical behavior of each species is distinctly different, yet almost all P at the
76 Earth's surface is present in an oxidised state (P^{5+}). Crustal P^{5+} is hosted by the mineral apatite
77 ($Ca_5[PO_4]_3[OH,Cl,F]$) in most crustal rocks. The poor solubility of this phase at ambient surface
78 conditions is widely considered to be a crucial challenge facing prebiotic reaction pathways that
79 require high dissolved P concentrations to function (Schwartz, 2006). This issue has spurred
80 efforts to find either environmental conditions under which apatite is highly soluble (Burcar et al.,
81 2016; Toner and Catling, 2020), or alternative mineral sources of P that would have been
82 abundant on early Earth (Pasek et al., 2017). The probability that any given P-bearing phase may
83 have interacted with a specific prebiotic environment is dependent upon the nature of the early
84 Earth and the abundance of a given prebiotic mineral at the time. However, Earth history is
85 especially poorly constrained for the time period in which life is thought to have emerged. As
86 such, even strong experimental evidence that a P-bearing mineral may be useful in prebiotic
87 chemistry has little explanatory power without a firmer grasp on what was and was not
88 geologically possible on early Earth.

89
90 Here, we review what is known about P mineral diversity in modern and ancient terrestrial
91 settings, as well as in exogenous materials that deliver P to Earth's surface. We focus on
92 evaluating the formation conditions of each phase, in order to construct a time-series evolutionary
93 history of P mineralogy at Earth's surface. We examine which phases are likely to have been
94 available during the Prebiotic Era. By considering the environmental, tectonic, and geochemical
95 pre-conditions that go along with each phase, we are able to exclude some phases from
96 consideration entirely, as well as provide an assessment of prebiotic plausibility and utility in
97 other cases.

98

99 In this context, it is important to define what is meant by ‘early’, and to provide context for the
100 initial conditions of the Earth system, and their rate and direction of evolution towards the
101 present. We generalize our thinking to conservatively describe the ‘early Earth’ as encompassing
102 the first billion years of Earth history (4.5-3.5 Ga). The Hadean Eon refers to the point in Earth
103 history (4 Ga) beyond which there is essentially no preserved and exposed rock-record available
104 to study. The earliest putative evidence of life in the rock record, at > 3.85 Ga, is rapidly
105 approaching this boundary (Dodd et al., 2017). It is therefore becoming increasingly likely that
106 the origin of life occurred at some time during the Hadean Eon. The ‘Prebiotic Era’, then, refers
107 to whatever portion of the Hadean Eon was dominated by wholly prebiotic chemistry, as opposed
108 to any form of extant biochemistry. In this review, we refer most generally to the early Earth, as
109 well as more specifically to the prebiotic Earth, when discussing implications of our work for the
110 origin of life.

11

12 **Phosphorus pathways in planetary precursors**

13

14 We begin by tracing P through those processes that formed Earth. Materials formed at each stage
15 would have had the potential to interact with one another during the relevant timeframe for
16 prebiotic chemistry (i.e., circa 4.53-4.0 Ga). For example, molecules native to asteroids might not
17 form in situ in prebiotic terrestrial settings, but could have been transported to the early Earth’s
18 surface during impact events. The evolution of P cosmochemistry across Early Solar System
19 history is illustrated in Figure 1, concluding with the formation of Earth.

20

21 *Nebula-phase materials*

22

23 Details of P cosmochemistry occurring in the Interstellar Medium (ISM) and in star-forming
24 nebular gas clouds are currently scarce. Emission lines for the molecular species PO and PN have
25 been observed in the ISM (Mininni et al., 2018). The ISM itself is depleted in P relative to diffuse
26 molecular clouds and star-forming regions – most probably due to P freeze-out onto dust grains
27 (Lebouteiller et al., 2005), although the chemical nature of this dust-bound P is not yet properly
28 constrained. Regardless, this expected reservoir is often suggested to act as a P source during dust
29 cloud collapse, star-formation, and the development of proto-planetary disks, with P being
30 released to the gas phase during heating associated with these processes (Lebouteiller et al.,
31 2005). The vast majority of nebular P is thus reprocessed during chemical partitioning into the
32 disk, reducing the prebiotic relevance of pristine nebular P-bearing species.

33

34 *Disk-phase materials*

35

36 Gas phase chemistry in the disk is complex, varies significantly with temperature, and hence also
37 varies with stellar distance and with time. The highest temperature at which P will condense to
38 form a solid phase is 1248 K (Lodders, 2003). At this temperature, reaction of nebular gas species
39 with already-formed native iron (Fe; e.g., in dust) results in the near wholesale removal of P from
40 the gas-phase in around 10,000 years. This process triggers schreibersite (Fe_3P) formation when P
41 reached a critical concentration of ~ 1 wt % in the metal (Pasek, 2019a; Pirim et al., 2014).
42 Schreibersite is often observed to be non-stoichiometric, with $\text{P} < 1$ atom per formula unit (Pasek,
43 2019a; Zanda et al., 1994). These Fe[P] phases comprise the oldest P-bearing minerals to form in
44 the Solar System and provide a starting point for tracking how P mineralogy may have evolved
45 over the next 4.5 billion years. Secondary reprocessing of disk materials then set the redox state
46 and concentration of P in asteroids and planetesimals, which were subsequently accreted to form
47 the Earth. These materials continue to be sampled and delivered to Earth today by meteorites,

48 providing us with a constraint on the minerals that may also have been delivered to Earth during
49 its Prebiotic Era.

50
51 **Phosphorus mineral diversity in meteorites**

52
53 Phosphide, both as a minor-components in Fe-metal and as individual mineral phases, dominates
54 in enstatite chondrites, as well as carbonaceous and ordinary chondrites that did not experience
55 significant aqueous or thermal metamorphism. However, given the sheer rarity of unaltered
56 chondrites, we do not consider this reservoir separately in our compendium of meteorite P data
57 (Table 1). Thermally metamorphosed and aqueously altered chondrite classes contain oxidised
58 phosphate minerals – in particular merrillite and members of the ternary end-member OH/F/Cl-
59 apatite series (Table 1). Oxidation was likely mediated by metasomatism following the
60 mobilization of early condensed ices into fluids and vapours, which was either driven by early
61 metamorphism and/or impact-heating events (McSween and Labotka, 1993; Zhang et al., 2016).

62
63 Phosphides also dominate in iron-rich reducing achondrites (Table 1), whereas phosphate
64 minerals dominate in more oxidizing silicate-rich achondrites (Table 1). Primary phosphates may
65 co-exist with phosphide phases in pallasite (‘stony-iron’) meteorites (Buseck, 1977). It has also
66 been suggested that a phosphide-fluid reaction sequence explains the presence of phosphorylated
67 carbon compounds in comets, e.g., Wild 2 (Brownlee et al., 2012) and in the organic-rich
68 carbonaceous chondrites (CCs), e.g., Murchison (Graaf et al., 1995). All of the materials indicated
69 in Table 1 and Figure 1 have the potential to have interacted with Earth surface and therefore set
70 in-motion different pre-biogeochemical processes. However, in practice, this prebiotic potential is
71 sensitive to the relative and absolute abundance of these phases, as well as the constraints
72 imposed by inherently stochastic delivery during impact bombardment.

73

74 **Modern exogenous fluxes**

75

76 The flux of meteoritic minerals to Earth must have been greater in the past than it is today, with
77 planetary bombardment being at its height during the Hadean Eon (4.5 to 4.0 Ga) and, most
78 likely, during the overlapping Prebiotic Era (Marchi et al., 2014). Acknowledging this, we will
79 now review and assess evidence pertaining to the composition of objects involved in Earth's early
80 impact history.

81

82 One means of evaluating the significance of exogenous P delivery (relative to endogenous
83 weathering sources) is to quantify and extrapolate modern meteoritic fluxes to Earth. The data
84 necessary to perform this analysis are given in Table 1, which lists the major meteorite classes,
85 the reported diversity and relative abundance of P-bearing minerals found in each, and the relative
86 abundances of these different meteorite classes in our collections. It should be noted that some of
87 these classes have been argued to be under-represented compared to the fraction of material by
88 mass that actually falls to Earth, because of preservation bias, e.g., a bias against preserving easily
89 weathered irons or pallasite meteorites (Binzel et al., 1993). Otherwise, however, we assume that
90 the relative abundances of material present in collections is a reasonable proxy for the material
91 flux to Earth now.

92

93 We systematically assembled available data regarding the number and mass abundance of
94 meteorites of all major classes present in global collections (Table 1). We combined these data
95 with estimates for the average P content of each class, as determined using data taken from
96 Metbase (<https://metbase.org>). We exclude minerals produced exclusively during terrestrial
97 weathering. Errors is propagated for both fall statistics and geochemical compositions. Literature

98 reports were also used to constrain the mineralogy, and thereby speciation, of P within each
99 meteorite class. However, owing to a general lack of quantitative data for this parameter, we are
00 forced to use a simplified relative abundance classification scheme, namely: common (0.1), minor
01 (0.01), rare (0.001), and very rare (0.0001). These are estimates, not measurements, and thus
02 cannot be associated with error terms. However, we note that these approximations are likely to
03 be reasonable upper bounds: the most likely deviation is that minor to very rare phases are
04 relatively much rarer than we have assumed. We consider schreibersite as synonymous with
05 primitive P-bearing metal in constructing our estimates of exogenous mineral flux.

06
07 Figure 2 illustrates a ranked P mineral flux to Earth based on mean P content. Phosphorus
08 delivered as schreibersite comprises the largest fraction of all exogenously delivered P minerals
09 (45.1 %), followed by the relatively insoluble phases merrillite (19.2 %) and apatite (15.4 %). The
10 high mass fraction of schreibersite is due mainly to its presence in iron meteorites, which make up
11 50.4 % by mass of known falls. The remaining 20 % of exogenously delivered P is dominated by
12 the more abundant phosphate minerals found in achondrites: sarcopside ($[\text{Fe}^{2+}, \text{Mn}^{2+}, \text{Mg}]_3[\text{PO}_4]_2$),
13 johnsomervilleite ($\text{Na}_3\text{CaFe}_{11}[\text{PO}_4]_9$), graftonite ($[\text{Fe}^{2+}, \text{Mn}^{2+}, \text{Ca}^{2+}]_3[\text{PO}_4]_2$), and stanfieldite
14 ($\text{Ca}_7\text{M}_2\text{Mg}_9(\text{PO}_4)_{12}$).

15
16 The estimated flux of all other P phases is relatively minor by comparison (3.8 %), but is again
17 dominated by phases found in irons – this time a more even split between oxidised and reduced P
18 minerals, followed by a wealth of rare phases present in abundances much less than 1 %. Overall,
19 we estimate that the modern meteoritic P flux is evenly split phosphide and phosphate (45.9 vs
20 54.1 % – Fig. 2). Phosphate delivery is somewhat diverse (5 major phases), whereas phosphide
21 delivery is overwhelmingly dominated by schreibersite.

22

23 An important caveat for these results is the potentially changing nature of accreting impactor
24 populations over time. For example, several recent models suggest that enstatite a/chondritic
25 material contributed more substantially to early exogenous fluxes (Piani et al., 2020; Sikdar and
26 Rai, 2020). Enstatite-like material is highly reducing and hence has schreibersite dominated P
27 mineralogy (Table 1). Enstatite-dominated models of early accretion will therefore predict
28 schreibersite-dominant early accretion fluxes, favoring exogenous delivery as a source of reduced
29 P on early Earth.

30
31 We lack errors on the modal abundance of P phases within each meteorite class. However,
32 obtaining new estimates of mineral modes is unlikely to change our presented results by
33 orders of magnitude. Nonetheless, the present values should not be taken as final estimates,
34 especially for rarer species. Overall, given that merrillite, apatite, and schreibersite dominate
35 within each meteorite class that has so far been observed, these phases must also have dominated
36 specific P mineral fluxes to the Earth's surface over time.

37
38 **Phosphorus pathways during planetary evolution**

39 *Planet formation*

40 Phosphorus availability at a planetary surface is dependent both on its concentration and redox
41 speciation. An important initial question to resolve is therefore: what was the relative abundance
42 of P in its different redox states at the Earth's surface in the aftermath of its formation?

43 The phosphorus content of the Earth cannot be assumed from cosmic abundances. Phosphorus is a
44 moderately volatile element, with a condensation temperature of 1248 K (Lodders, 2003), and
45 therefore may not have fully condensed at Earth's heliocentric distance. Instead, the P content of
46 the Bulk Silicate Earth (BSE) is estimated from its correlation with a non-volatile (refractory)

47 element (e.g., Nd) in mantle-derived basalts (Mallmann and O'Neill, 2009; Palme and O'Neill,
48 2014). The P content of the BSE is depleted beyond the extent that volatility alone can explain
49 (Fegley and Lewis, 1980; Palme and O'Neill, 2014; Schönbächler et al., 2010). This additional
50 depletion occurs because P can exhibit siderophile behaviour, causing it to partition into a planet's
51 iron-rich core (Righter et al., 2018, 2010).

52 Although P's chemistry means it is partially lost to Earth's core ($> 80\%$ – Fig. 3), during mantle
53 melting it behaves as an incompatible element and is concentrated into mantle melts.
54 Consequently, most newly formed crust is P-enriched relative to the mantle (Figures 1,3). Modern
55 oceanic and continental crust together represent $> 30\%$ of all P in the BSE (Fig. 3). This
56 enrichment was likely established early, with early crustal P estimated at 100-1000 ppm in early
57 Hadean crust vs. 87 ppm in BSE (Cox et al., 2018; Jenner et al., 2013; Keller and Schoene, 2012;
58 O'Neill and Jenner, 2012; Palme and O'Neill, 2014). Overall, crustal P abundances would not
59 have differed all that greatly from primitive planetary building blocks, such as chondritic
60 meteorites (Palme and O'Neill, 2014). However, the oxidation state of early crustal P likely
61 differed strongly from that of Earth's accretionary building blocks.

62 At equilibrium, P partitioned into a metal phase speciates as reduced P^0 , as well as P^{-1} , (Pirim et
63 al., 2014), whilst P left in the silicate fraction is oxidised (P^{5+}). Experimental constraints on
64 conditions relevant to an early terrestrial magma ocean highlight that even the most reducing
65 conditions consistent with the observed end-stage chemistry of the upper mantle would still
66 stabilise oxidised P^{5+} in silicate melts (Righter et al., 2018). However, we can expect reduced P
67 will be found dissolved in native iron equilibrated with mantle silicates (Zanda et al., 1994). We
68 can estimate the magnitude and redox speciation of P in modern solid Earth reservoirs by
69 combining estimates of bulk reservoir P concentration; phase abundances in the crust, upper
70 mantle, transition zone (TZ), lower mantle, and core; and experimental constraints on P

71 partitioning behavior between metallic and silicate liquids/minerals (see Supplementary
72 Information and Supplementary Table 1) (Broska and Petrik, 2008; Brunet and Chazot, 2001; Cox
73 et al., 2018; Frost et al., 2004; Gale et al., 2013; Haggerty et al., 1994; Huang et al., 2013;
74 Kaminsky, 2012; McDonough and Sun, 1995; Palme and O'Neill, 2014; Righter et al., 2010;
75 Taylor and McLennan, 1995; Zhu et al., 2019).

76 Whilst P partitions strongly into native iron metal compared to silicates (Righter et al., 2010), low
77 metal abundances nonetheless result in a silicate-dominated P reservoir throughout much of the
78 BSE. We find that reduced (metal-bound, siderophile) P is largely absent in the BSE, first
79 appearing as a minor reservoir (< 0.01 %) with the onset of native iron metal saturation below 250
80 km depth in the upper mantle, and only increasing to account for around 0.01 % of lower mantle
81 P and finally > 99 % of core P (Fig. 3). Based on these calculated low reduced P abundances and
82 the rarity of upper mantle material exposed at Earth's surface today (Hart et al., 1990), it is
83 unclear that these deeply buried reduced P reservoirs could ever interact with surface
84 environments. Overall, the endogenous mineral-hosted P available to prebiotic chemistry would
85 have been left entirely in an oxidised redox state following planetary differentiation.

86 The key point for the early P cycle is that the thermodynamics of core and crustal formation do
87 not produce scarcity in bulk P. Instead, scarcity is created in terms of reactive (reduced) P. This
88 leads to planetary crusts that broadly lack reduced P species and instead contain only relatively
89 'insoluble' phosphate (P^{5+} ; Fig. 1). No phase is entirely insoluble, and even phosphate-containing
90 minerals will contribute P to lakes, rivers, and the oceans. The relative abundance of these
91 oxidised P-bearing phases at the surface of prebiotic Earth will have been controlled by the
92 composition and geodynamics of the early crust.

93 *Crustal evolution*

94 The two most important P-hosting phases in Earth's crust are fluorapatite ($\text{Ca}_5[\text{PO}_4]_3\text{F}$) and
95 olivine ($[\text{Fe},\text{Mg}]_2\text{SiO}_4$) (Schwartz, 2006; Tollari et al., 2006; Toplis et al., 1994; Watson, 1980).
96 Whilst phosphorus is moderately incompatible in olivine, apatite is highly soluble in typical
97 mantle melts (Green and Watson, 1982; Watson, 1980; Watson et al., 2015). Phosphorus
98 accumulation and Si-enrichment during extended fractionation crystallization will push melts
99 towards apatite saturation (Watson, 1980). Apatite is therefore broadly absent in relatively Si-
00 poor and P-poor rocks, e.g., large swathes of the upper mantle and oceanic crust (Brunet and
01 Chazot, 2001; Haggerty et al., 1994), whilst most continental crustal rocks are apatite saturated
02 (Watson, 1980). Apatite may contain > 95 % of all continental crustal P (Jahnke, 1992; Paytan
03 and McLaughlin, 2007), and thus a large fraction of all crustal P (Fig. 3). This relationship
04 between crustal composition and P mineralogy allows us to link the near-surface P mineralogy of
05 the prebiotic Era to the composition of early crust.

06 The concept of non-uniformitarianism which has gained such traction in thinking about
07 exogenous P fluxes to the early Earth may also be relevant for endogenous sources. At a global
08 scale, crustal compositional evolution can broadly be described by two end-member scenarios
09 (Fig. 4):

10 (A) A voluminous and broadly ultramafic-mafic (Si-poor) proto-crust (Dhuime et al., 2017, 2015;
11 Hawkesworth and Jaupart, 2021), in which apatite is mostly absent and P is hosted mainly by
12 olivine.

13 (B) Large volumes of relatively felsic (high Si) and apatite-dominated continental crust along
14 with a more mafic (broadly apatite undersaturated) oceanic crust (Korenaga, 2018; Lipp et al.,
15 2020; Rosas and Korenaga, 2018).

16 These are all strikingly different views of the Early Earth – and yet, all are currently permissible
17 within the bounds of available constraints from rheological and thermal models as well as
18 composition-age plots of crustal rocks. For example, fine-grained sediments, which formed
19 during the weathering of crustal material across large surface areas, have been used as a proxy for
20 crustal average composition (Rudnick and Gao, 2014). Depending on the chemical proxies one
21 chooses to focus on, however, as well as the way that various possible biases are accounted for
22 (e.g., chemical alteration of sediments), the same data can be interpreted as reflecting a more
23 mafic or similarly felsic upper continental crust in deep time (Greber et al., 2017; Greber and
24 Dauphas, 2019; Tang et al., 2016). Non-chemical proxies, e.g., heat flow, and isotopic mass
25 balance models provide alternative means to reconstruct the nature of early crust (Hawkesworth
26 and Jaupart, 2021; McCoy-West et al., 2019), with recent work favoring large volumes of mafic
27 crust (i.e., end-member Model A). Overall, early crustal chemistry is uncertain. However, within
28 that uncertainty, there remains the distinct possibility that early crustal P reservoirs were not
29 apatite-dominated.

30 Although apatite and silicate phases are the dominant P reservoirs in the modern crust,
31 phosphorus mineralogy is highly diverse. Over 600 separate species in which P is a stoichiometric
32 component are currently listed in the Mineral Evolution Database (MED; ruff.info/ima/). We can
33 assess the interplay of tectonic, compositional, and crustal regimes in the context of early P
34 mineral diversity by leveraging recent advances in the study of accessory mineralogy –
35 specifically, the Mineral Evolution Database. This fine-scale heterogeneity of crustal P
36 mineralogy is potentially important to consider in the case of prebiotic chemistry, as even globally
37 rare phases may be locally abundant and therefore relevant to small-scale environmental
38 processes leading up to the origin of life.

39
40 *The Mineral Evolution Database*

41

42 Accessory P minerals are often difficult to model thermodynamically and also lack specific
43 experimental and field investigation. Recently, however, large-scale datasets that specifically
44 describe the accessory mineralogy of exposed crustal rocks have become available (e.g., the
45 Mineral Evolution Database – MED). The Mineral Evolution Database (<http://rruff.info/ima/>), in
46 association with mindat (<https://www.mindat.org>), combines spatial (locality) with temporal (age)
47 data for individual mineral occurrences on Earth (Grosch and Hazen, 2015; Hazen, 2013; Hazen
48 et al., 2008; Hystad et al., 2019; Morrison et al., 2018). For this study, we processed MED data
49 for all of the P minerals so far used in prebiotic experiments, as well as additional instances of
50 phosphates that might come under future scrutiny in this context.

51

52 Phosphorus Mineral Evolution Database (PMED) age data is sourced from the literature on
53 specific mineral-locality occurrences listed on mindat.com and <http://rruff.info/ima/>. These ages
54 can be of any kind – from isotopic to stratigraphic. Age data has been carefully filtered on the
55 basis of paragenesis for this work i.e., high temperature primary vs low temperature secondary
56 species. This provides greater certainty that meaningful age data is being interpreted in each case.

57

58 The temporal resolution of PMED declines in step with the rock record, terminating at 4 Ga. It is
59 therefore challenging to obtain a representative dataset of occurrence over Earth history for each
60 mineral. Compounding this problem, many of the phases of interest are short-lived under
61 ‘ambient’ conditions; not surviving diagenesis, lithification, metamorphism, or weathering. It is
62 especially challenging to compile accurate age distributions for these phases. Therefore, for those
63 species that derive from more stable primary phases, the age relationships of parental minerals
64 and suitable environmental conditions for their alteration have also been ascertained. This

65 approach helps to extend the temporal range of known mineral localities where specific P-phases
66 of interest could have formed.

67
68 *Phosphorus mineral evolution*

69
70 In this work, we have evaluated the paragenetic relationships and prebiotic plausibility of all
71 phosphorus-bearing mineral species in PMED. Should the reader wish to check the details of a
72 candidate mineral that is not discussed here, all of the information equivalent to that reported in
73 this article is available online at med.com, mineralweb.com and handbookofmineralogy.com. 65
74 separate mineral species were targeted for detailed investigation, all of which are of some
75 relevance to the question of early Earth phosphorus availability. This set contains either phases
76 that have been previously used in ‘prebiotic’ chemistry, or that have formation conditions of some
77 potential relevance to early Earth.

78
79 Table 2 presents compiled data on P mineral host lithology, oldest occurrence, number of
80 occurrences, and conditions of formation for P-bearing phases of prebiotic interest. These data
81 can be used to assess which mineral species plausibly existed in the Prebiotic Era, and then, of
82 those species, which (if any) have any notable potential for driving prebiotic chemistry. We
83 further classify those species according to the tectonic settings in which the environmental
84 conditions needed for their formation occur. This nuance becomes important when considering
85 that accessory phosphate mineralogy is diverse and will vary hugely between the different rock
86 types that characterize different tectonic models. Doing so allows us to draw a link between the
87 early geological state of prebiotic Earth and (mineralogical) aspects of origin of life scenarios.
88 This link is crucial, since large scale tectonic processes will have behind a deeper imprint than

89 minor environmental settings in the sparse geochemical evidence with which we are left to
90 reconstruct prebiotic Earth.

91

92 A major subdivision can be made on the basis of crustal composition, given that stagnant and
93 active tectonics result in the production of more mafic and more felsic rocks, respectively. A
94 secondary division of active tectonic mode is then made. We therefore extend the compositional
95 scenarios A (mafic) and B (felsic) given in Figure 4, and discussed earlier, into the following
96 tectonic categories: a primitive regime with stagnant lid tectonics and mafic crust (Fig. 5A), an
97 evolved regime with vertical sagduction tectonics and some felsic continental crust (Fig. 5B-1),
98 where dense hydrated crustal material moves back into the mantle in downward moving diapirs,
99 and an alternative evolved regime, equivalent to the one operable on Earth today, of horizontal
00 subduction-driven plate tectonics (Fig. 5B-2).

01

02 In Model B-1, early continental crust was generated via cyclic vertical sinking and melting of
03 hydrated mafic crust (Johnson et al., 2017). In Model B2, continental crust is produced by the
04 vertical passage of mafic rocks beneath an overriding plate of material i.e., slab subduction. Slab
05 dehydration then results in high-pressure hydrous melting of overlying crust and arc mantle (Fig.
06 5B-2). Specifically, invoking material formed only in an e.g., subduction regime in a prebiotic
07 model then requires the early Earth to have hosted such settings.

08

09 Those species whose environmental conditions of formation involve processes that are
10 definitively known to have developed at some point after the Hadean Eon are filtered out
11 (highlighted in red). For example, pseudomalachite forms only via oxidative weathering and
12 hence can only have occurred since the Great Oxygenation Event (GOE), at ~ 2.45 Ga (Table 2).
13 Despite this inherent limitation, pseudomalachite has been used as a mineral-phosphorylating

14 agent in some prebiotic experiments (Costanzo et al., 2007). Whilst results from these projects
15 still have relevance for highlighting potential chemical avenues of interest, they cannot provide
16 outright solutions to the problem of concentrating P on early Earth given their use of materials
17 that did not plausibly occur in the Hadean Eon.

18
19 We can rule out a number of other similar mineral species as prebiotically relevant based on their
20 paragenetic associations (Table 2). Whilst ages of oldest occurrence are challenging to ascertain
21 for secondary species, we can confidently identify these ages for primary igneous species. For
22 example, minerals containing oxidised Fe^{3+} as a stoichiometric component occur only after 2.45
23 Ga. This outcome adds confidence to any inferences about secondary species made solely on the
24 basis of paragenetic mode.

25
26 The potential of each phase in Table 2 for driving prebiotic chemistry is dependent on its
27 abundance, reactivity, and complementarity to a prebiotic chemical model i.e., reaction schemes
28 that are proposed to have operated in hot springs, submarine vents, etc. Several species in Table 2
29 can be identified as extremely rare – with only a few occurrences present in the entirety of the
30 database (highlighted in purple). These mineral species may simply occur under very unusual
31 environmental circumstances, be prone to preservation bias, or some combination of the two. A
32 key example is schreibersite which, being a phosphide mineral, will have suffered from oxidative
33 weathering at the Earth's surface since the GOE, whilst also require unusual reducing conditions
34 for its formation. There are then those species which were both plausibly present in the Hadean
35 and likely to have been abundant at the time, but which have thus far proven essentially
36 completely unreactive for prebiotic chemistry, e.g., xenotime and monazite (Pasek et al., 2017).
37 These highly insoluble and unreactive P minerals are highlighted in blue. Until new experiments

38 prove otherwise, these species can be considered essentially irrelevant as mineral sources of
39 prebiotic P. ‘Likely’ Prebiotic phases are highlighted in green and ‘uncertain’ phases in orange.

40

41 Many of the primary species highlighted here as of ‘uncertain’ prebiotic occurrence form in
42 sagduction or subduction regimes (Fig. 5B-1/2). Triplite, hydroxylherderite, vivianite,
43 whitlockite, and herderite are known to occur (as igneous phases) in granitic pegmatites, which
44 result from extreme fractional crystallization and differentiation (Table 2). There is currently little
45 evidence that granite pegmatites occur in the rock record beyond ~ 3 Ga (Sweetapple and Collins,
46 2002). Preservation bias of these relatively rare lithologies might be invoked to explain their
47 absence in the early Archean rock record, yet it is also contentious whether or not the geodynamic
48 conditions required to produce them could have prevailed much before this time. Pegmatites are
49 found in I-A-type (igneous-derived) and S-type (sediment-derived) felsic magmatic suites.

50

51 For I-A-type pegmatites (igneous source materials), it would appear that the concentration of
52 heat-producing and volatile elements due the recycling of continental crust is important for their
53 formation, requiring an evolved geodynamic regime (Fig. 5B-1/2). A key pre-requisite for S-type
54 granite formation is melting of metasedimentary material, along with subsequent fractionation
55 (enhanced by the presence of volatiles). This melting often occurs in subduction-related orogens
56 (London, 2018). S-type granites are therefore most plausible given some form of tectonic cycling
57 of volatiles from the surface to depth (Fig. 5B-1/2). Hence, we can tie the presence or absence of
58 pegmatitic mineral species on Early Earth to prevailing tectonic regimes. Pegmatitic species are
59 unlikely to have occurred on an early Earth with stagnant lid tectonics (Fig. 5A) – regardless of
60 whether some low-volume felsic magmatism was ongoing.

61

62 Although several of the rare accessory phases of plausible prebiotic occurrence in Table 2 have
63 been shown to have some unique/useful role in experimental work, there is no strong case that
64 they were abundant on early Earth – limiting the plausibility of prebiotic scenarios that rely on
65 such phases. This leaves several species which, on the basis of available evidence, are plausibly
66 prebiotic, possibly abundant, and potentially soluble.

67

68 **Phosphorus mineralogy and prebiotic P availability**

69

70 *Schreibersite*

71

72 Schreibersite is a promising candidate for a prebiotic source of P owing to its high reactivity and
73 solubility in natural waters of varied composition at ambient conditions (Bryant et al., 2013; Kee
74 et al., 2013; Pasek, 2019b; Pasek et al., 2015, 2013, 2007; Pasek and Lauretta, 2008), yet is very
75 rare in the terrestrial rock record (Table 2). For schreibersite to be a primary igneous mineral on
76 early Earth requires that magmas were forming under exceptionally reducing conditions (Brett
77 and Sato, 1984) – far more reducing than any conditions found on the modern Earth. However,
78 Earth's upper mantle likely oxidised to near its modern state very rapidly (Trail et al., 2011;
79 Williams et al., 2012; Yang et al., 2014), and (possible) reduced deep mantle P reservoirs are
80 unlikely to have interacted with surface reservoirs.

81

82 It is conceivable that localised reducing zones of the upper mantle and crust could have occurred
83 as 'hold-overs' from highly reducing conditions that prevailed during Earth's formation, or were
84 generated during reducing events, e.g., the impact of a large enstatite-type body (Benner et al.,
85 2020). H₂-rich magmas generated from these reducing source materials may have migrated
86 towards the surface and hence provided a flux of reducing material to the surface for up to several

87 hundred million years (Bali et al., 2013; Rimmer and Shorttle, 2019). These putative reducing
88 magmas may well have become saturated in reduced P minerals, or Fe-P alloys. Similarly, such
89 ultra-reducing localized settings may provide a plausible host environment for alternative
90 phosphide phases, e.g., Table 2 (Britvin et al., 2015) and reduced P compounds, e.g.,
91 cyclophosphates (Britvin et al., 2020), which would otherwise appear to require the involvement
92 of biology (Table 2). The plausibility of hydrothermal reduced-P-bearing systems is deserving of
93 future study (Fig. 6).

94
95 Even more plausible is exogenous schreibersite delivery. Our review of meteoritic mineralogy
96 strongly supports that this phase would have been among the most abundant P-bearing phases
97 delivered to early Earth. However, unlike the other phases with strong prebiotic potential
98 discussed in this review, schreibersite availability would have been stochastic. Direct delivery
99 would only have been possible where impactor velocity and size permitted passage through the
00 atmosphere and also avoided vaporization upon arrival at the surface. Indirect alternatives for
01 exogenous reduced P delivery include settling of post-ablation vapor condensates (Douglas et al.,
02 2020; Mehta et al., 2018) and production of reduced P in-situ, in impact craters (Pasek, 2017).
03 The plausibility of prebiotic chemistry utilising these various exogenous sources of P has yet to
04 receive detailed attention (Fig. 6).

05
06 A key concern regarding the prebiotic utility of reduced-P-bearing phases is their solubility in
07 aqueous solution. Direct surface-reactivity during schreibersite corrosion is known to actively
08 phosphorylate organic compounds (Pasek et al., 2007). However, the dissolution rate and ultimate
09 steady-state concentrations of reactive P in environments that may have interacted with reduced-
10 P-bearing phases remain unknown. These constraints will be critical for evaluating the role that
11 reduced-P-bearing phases may have played in prebiotic chemistry, which may have required up to

12 molar concentrations to ensure effective pH buffering and selective forward reactions (Patel et al.,
13 2015; Sutherland, 2015).

14

15 *Apatite*

16

17 The apatite ternary end-members stand out as the most abundant phosphate phases listed in
18 PMED. The presence of these phases in preserved early felsic igneous rocks (Table 2) confirms
19 the likelihood that apatite, principally as F-bearing fluorapatite (Watson, 1980), would have
20 comprised at least some non-trivial fraction of the crustal P reservoir. Apatite has a very low
21 solubility in the majority of solutions found at the Earth's surface today (Brantley and Olsen,
22 2014). However, there are in fact several of ways to drastically increase apatite solubility. These
23 mechanisms include site-specific chemical attack by cations, increased temperature, and physical
24 weathering (Chaïrat et al., 2007; Harouiya et al., 2007). The most dramatic and universally
25 relevant control on apatite solubility is pH (Pearce, 1988). Apatite dissolution rate and solubility
26 product increase by orders of magnitude across both the temperature and pH scales, implying that
27 aqueous environments of $> 20\text{ }^{\circ}\text{C}$ and $< \text{pH } 7$ will readily dissolve out apatite during water-rock
28 interactions (Chaïrat et al., 2007; Strachan, 2017).

29

30 Experiments have also revealed high sensitivity of fluorapatite stability to the dissolved inorganic
31 carbon (DIC – in seawater, an equilibria between carbonic acid, bicarbonate ion and carbonate
32 ion) content of aqueous fluid in equilibrium with a source of CO_2 (Jahnke, 1984). In experiments
33 reported by (Pan and Darvell, 2010, 2009), the solubility effect of pCO_2 on apatite was detectable
34 even at very low pH i.e., effectively zero carbonate ion in solution. The authors attributed this
35 continued effect on apatite solubility to complexation of Ca by bicarbonate (HCO_3^-) and carbonic
36 acid in solution, whilst noting that the DIC effect is largest at high pH. Overall, the results of (Pan

37 and Darvell, 2010, 2009) imply that $p\text{CO}_2$ is a relevant factor in controlling apatite solubility
38 regardless of pH. We therefore expect inorganic carbon to have played an important role in
39 solubilising apatite across a wide range of geochemical environments (Kakegawa et al., 2002).
40 Overall, experimental constraints suggest that apatite will be most useful as a prebiotic P source
41 in end-member scenarios where both global surface temperatures and atmospheric $p\text{CO}_2$ are high.

42
43 Apatite is also among the most common exogenously delivered P-bearing phases (Fig. 2).
44 Exogenous apatite does not obviously have a clear advantage over endogenous apatite for fueling
45 high P availability during prebiotic chemistry (Table 3). A circumstance in which this situation
46 would be reversed is given a putative mafic early crust (Fig. 5A; Fig. 6; Table 3), where
47 endogenous silicate- and exogenous apatite-hosted P were both more available than the crustal
48 apatite P reservoir. Especially in earliest Earth history, then, and potentially during the origin of
49 life, it is possible that apatite may have only rarely occurred in the Earth's crust. In its stead,
50 silicate phases would have dominated the mass balance of available P in surface-exposed
51 environments.

52 53 *Silicate phases*

54
55 Silicate phases, whilst previously considered as exotic and reactive potential candidates for
56 supplying P to prebiotic chemistry (Holm, 2014), have received little attention in the context of
57 experimental prebiotic chemistry. However, silicate-hosted P may have dominated the crustal P
58 reservoir on an early Earth with little continental crust (Fig. 3-4). Crystalline mafic silicate phases
59 (e.g., olivine, pyroxene) are generally slower to weather than apatite, mafic silicate glasses are
60 comparatively rapidly broken down across a range of physiochemical conditions, and all of these
61 phases weather rapidly at high temperatures (Prigobbe et al., 2009). This perspective is important

62 for the plausibility of origin scenarios that rely on high P concentrations in submarine or subaerial
63 hydrothermal environments, where higher temperatures would serve to accelerate the dissolution
64 of crystalline and glassy mafic silicate phases.

65
66 A challenge in this regard, though, is that such models typically rely upon iron-oxide formation as
67 a critical part of the prebiotic chemical network (Barge et al., 2015). Such phases would act to
68 scrub phosphate from solution and thereby potentially impose local limits on P availability. On
69 the other hand, recent experimental work has shown that iron-redox chemistry may
70 circumnavigate these issues: sorbed phosphate may be reduced and released as phosphite during
71 hydrothermal alteration (Herschy et al., 2018) and/or prebiotic reactions involving P may take
72 place on iron-oxide mineral surfaces directly (Wang et al., 2019) (Fig. 6; Table 3).

73

74 **Conclusions and outlook**

75

76 *Limited diversity of P minerals on early Earth*

77

78 Despite the enormous diversity of P mineralogy observed today, mineral evolution indicates that
79 very of these minerals would have been present on the early Earth, with even fewer being
80 potentially important for prebiotic chemistry. Alongside silicate phases, in which P comprises a
81 minor component, only apatite is of clear relevance as an endogenous source of P for prebiotic
82 chemistry (Fig. 6; Table 3). Exogenous phases of importance are limited to merrillite, apatite, and
83 schreibersite (Fig. 6; Table 3).

84

85 We rule out a number of phases as being prebiotically plausible, some of which have previously
86 been used in prebiotic analogue experiments (e.g., pseudomalachite). This restricts the

87 mineralogical parameter space available for origin of life scenarios. This allows us to identify the
88 specific challenges or advantages of a given mineral-chemical scenario for prebiotic chemistry.
89 These issues are unique to each phase (Table 3). That the environmental conditions needed to
90 liberate P from each phase can differ so much suggests that distinct mineral-chemical-
91 environmental scenarios for prebiotic chemistry may be formulated (Table 3; Fig. 6). This
92 outcome is useful for reducing the parameter space of possible scenarios for prebiotic chemistry.
93 Moreover, a specific plausibility can be conferred to each scenario based on the assumed
94 distribution of mineral phases on early Earth. As such, a better understanding of early Earth
95 geology, chemistry, and surface environment will serve to clarify progressively the prebiotic
96 plausibility of these scenarios.

97

98 *Mineralogy and the probability landscape of prebiotic chemistry*

99

00 The plausibility landscape for elevated aqueous P concentrations on the prebiotic Earth heavily
01 depends on the assumptions we make about early P mineralogy. If specific rare minerals are
02 invoked in a chemical model, then the probability of that scenario is inherently limited by a
03 coincidence of geological processes and environmental conditions (e.g., rare pegmatite formation
04 followed by overlapping meteorite impact). Conversely, models that use species of global
05 distribution may have their probability mainly controlled by other factors, e.g., occurrence of
06 hydrothermal systems which promote P-mineral dissolution.

07

08 Looking again at globally distributed phases, a broadly mafic early crust will confer a
09 probabilistic advantage to models invoking mafic silicate phases, whereas a felsic early crust will
10 favor the involvement of (flour)apatite. We can therefore directly relate the probability of

11 mineral-chemical scenarios to the tectonic and environmental state of early Earth, bridging the
12 fields of geoscience and prebiotic chemistry.

13

14 This review has highlighted the importance of understanding long-term changes in Earth's
15 accreted materials, crustal composition, and tectonic mode when reconstructing early available P
16 mineralogy. Further constraints on early Earth P mineralogy will therefore help to discriminate
17 between competing models of prebiotic chemistry.

Acknowledgments

Acknowledgments: Dr Mahesh Anand, Dr Paul Rimmer, and Dr Sami Mikhail are thanked for encouragement and during the conception, researching and writing of this manuscript.

Funding: This research was funded by NERC, grant number NE/L002507/1, UKRI. Sloan, Deep Carbon Observatory, Keck, Templeton, NASA Astrobiology Institute, and a private foundation are all acknowledged for their support. F.J acknowledges funding from the NERC ‘Deep Volatiles’ consortium grant (NE/M000427/1). H.W. acknowledges funding from the NERC ‘Mantle Volatiles’ consortium grant (NE/M000303/1) and from the ERC Consolidator Grant 306655 (‘Habitable Planet’). M.P. acknowledges funding from NASA Exobiology grant 80NSSCC18K1288.

Author Contributions: Conceptualization, C.W., O.S., F.J., and R.H. methodology, C.W.; validation, C.W. and O.S. formal analysis, C.W.; investigation, C.W.; resources, O.S, H.W., and R.H.; data curation, C.W. and R.H.; writing—original draft preparation, C.W.; writing—review and editing, C.W, O.S, F.J., H. W, R.H., A.Z., S.M., J.G.; visualization, C.W. and O.S.; supervision, O.S, H.W.; project administration, O.S.; funding acquisition, C.W., O.S., M.P., R.H. All authors have read and agreed to the published version of the manuscript.

Competing interests: The authors declare no conflicts of interest.

Data and materials availability: : All data needed to evaluate the conclusions in the paper are present in the paper.

Figures and Tables

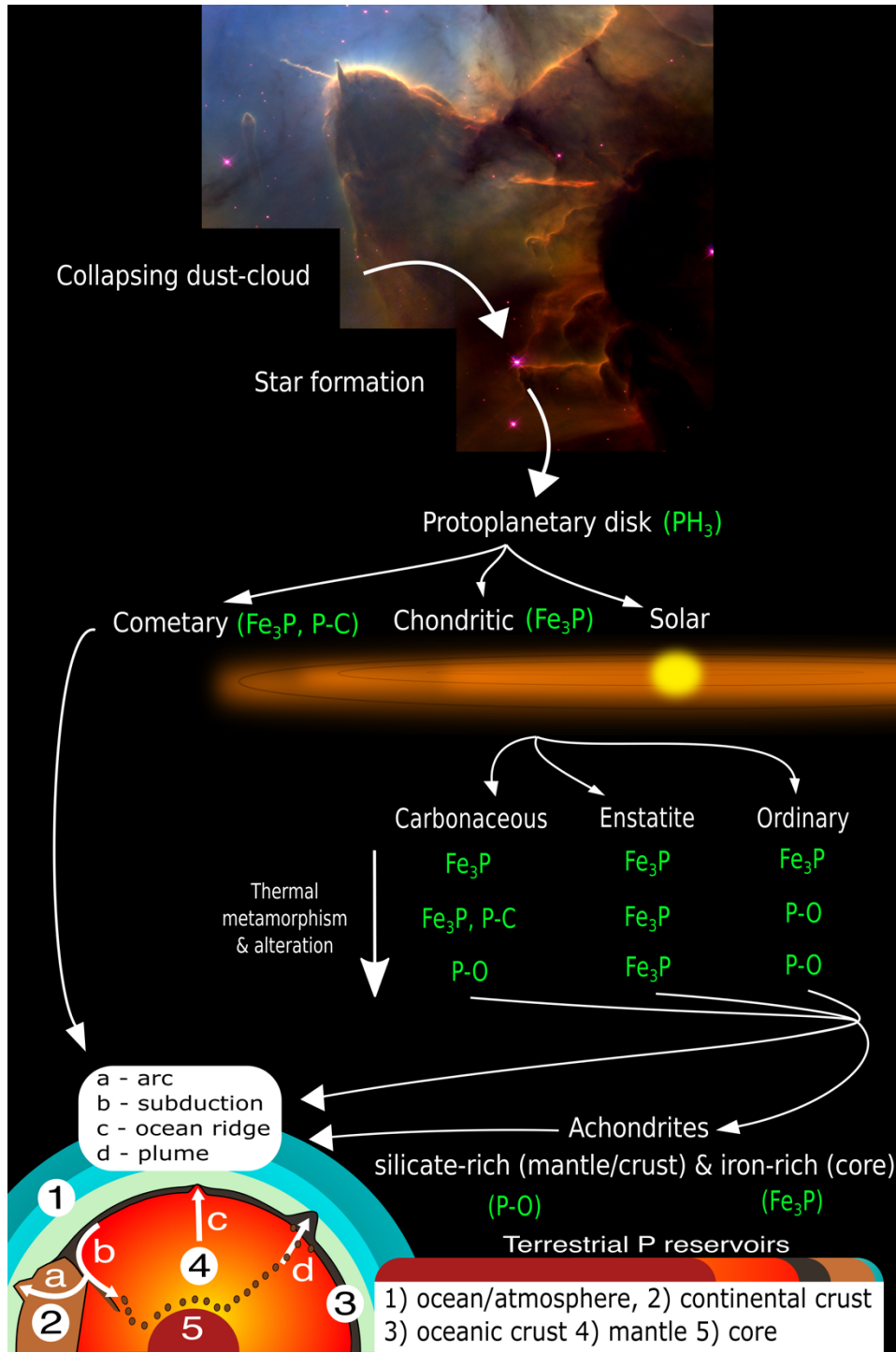


Figure 1: Pathways followed by P during early Solar System history. The early-Solar nebula would have condensed primarily reduced P as Fe_3P , both in comets and in chondrules (and hence chondrites). Thermal metamorphism and equilibration of chondrite parent bodies saw the oxidation of metal-bound P to form phosphate minerals. Following accretion of bodies large enough to experience melting, segregation of metal along with siderophile P to planet(esimal) cores created a dichotomy of reduced ‘inner’ P reservoirs and oxidised ‘outer’ reservoirs, i.e. core vs. mantle material. Color bar gives rough indication of P reservoir sizes: specific values are given in Figure 3.

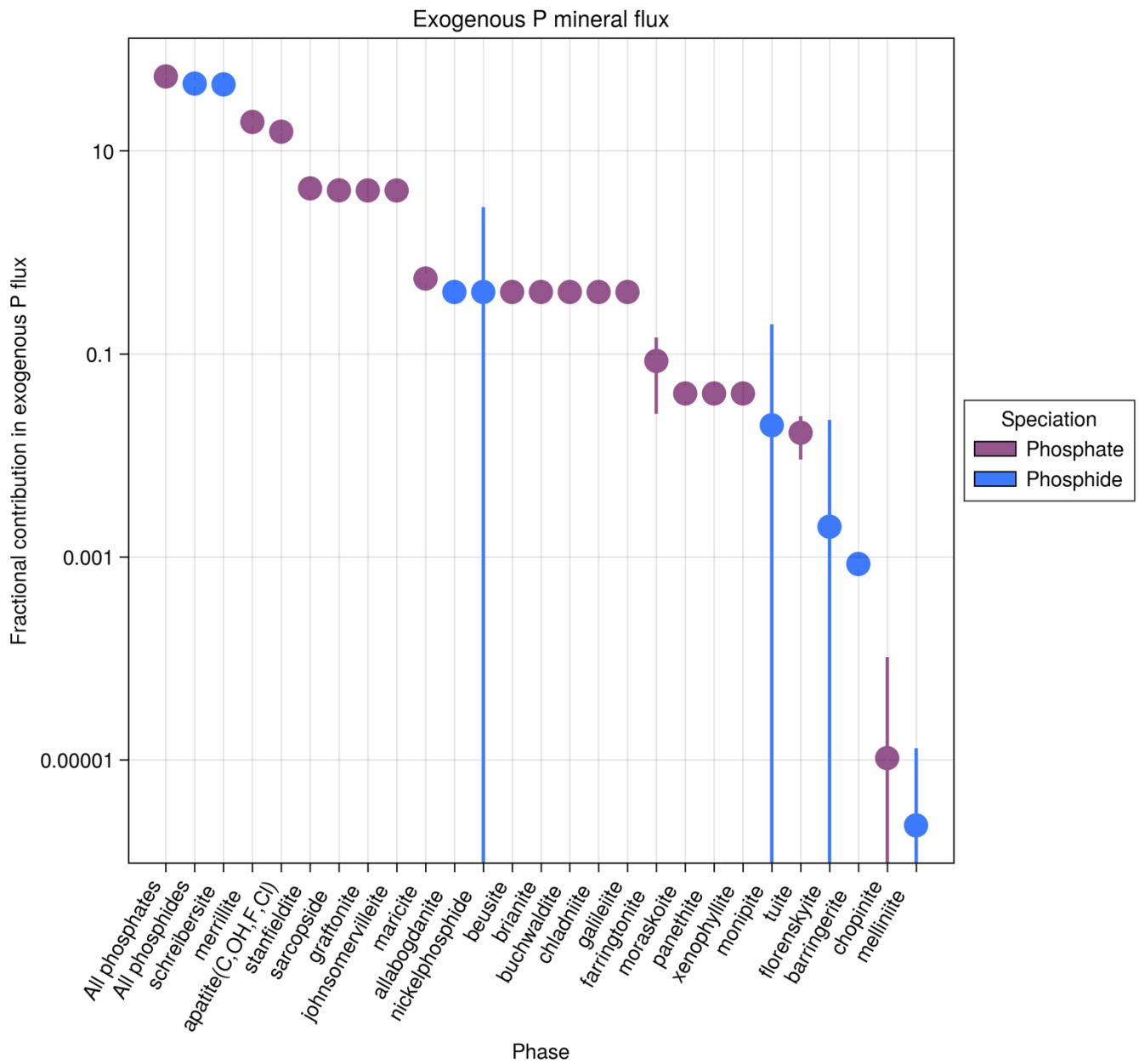


Figure 2: Percentage of total (modern) exogenous P flux represented by various mineral species. Also indicated is whether or not the mineral species occurred in terrestrial settings on the Hadean Earth. Red colored symbols indicate phosphate phases. Blue colored symbols indicate a phosphide phase. Error bars are 2 s. Data compiled from MetBase (December 2019).

Table 1: Phosphorus mineralogy of meteorites

Meteorite Class	P minerals (listed in order of decreasing abundance)	Fall statistics (mass %)	P content (ppm \pm 2 s)
Chondrites			
Ordinary	<i>OH/F/Cl-apatite, merrillite, maricite, tuite, phosphoran-olivine</i>	37.8	1100 \pm 58
Carbonaceous	<i>Schreibersite, OH/F/Cl-apatite, merrillite, monipite</i>	4.4	1280 \pm 100
Enstatite	<i>Schreibersite, perryite-nickelphosphide</i>	0.5	1260 \pm 224
Stony-irons			
Irons	<i>Schreibersite, stanfieldite-graftonite-sarcopside, johnsomervilleite, allabogdanite, brianite, maricite-nickelphosphide-beusite-buchwaldite-chladniite-chopinite-moraskoite-panethite-xenophyllite</i>	49.6	2340 \pm 391
Mesosiderite	<i>Merrillite, schreibersite, farringtonite</i>	1.2	2805 \pm 706
Pallasite	<i>Schreibersite, stanfieldite-howardite-merrillite-farringtonite, barringerite, phosphoran-olivine</i>	0.6	4140 \pm 6070
Asteroidal achondrites			
HEDs	<i>Apatite, merrillite,</i>	2.7	507 \pm 67
Aubrite	<i>Schreibersite</i>	2.4	291 \pm 2720
Angrite	<i>Apatite, merrillite</i>	0.003	618 \pm 146
Primitive achondrites			
Ureilite	<i>Schreibersite, Cl-apatite, merrillite</i>	0.01	693 \pm 292
Lodranite	<i>Merrillite, schreibersite</i>	0.002	1370 \pm 1770
Acapulcoite	<i>Schreibersite, merrillite</i>	0.004	1370 \pm 1770
Winonaite	<i>Schreibersite</i>	0.0003	1900 \pm 1340

Note: Data compiled from MetBase (December 2019)

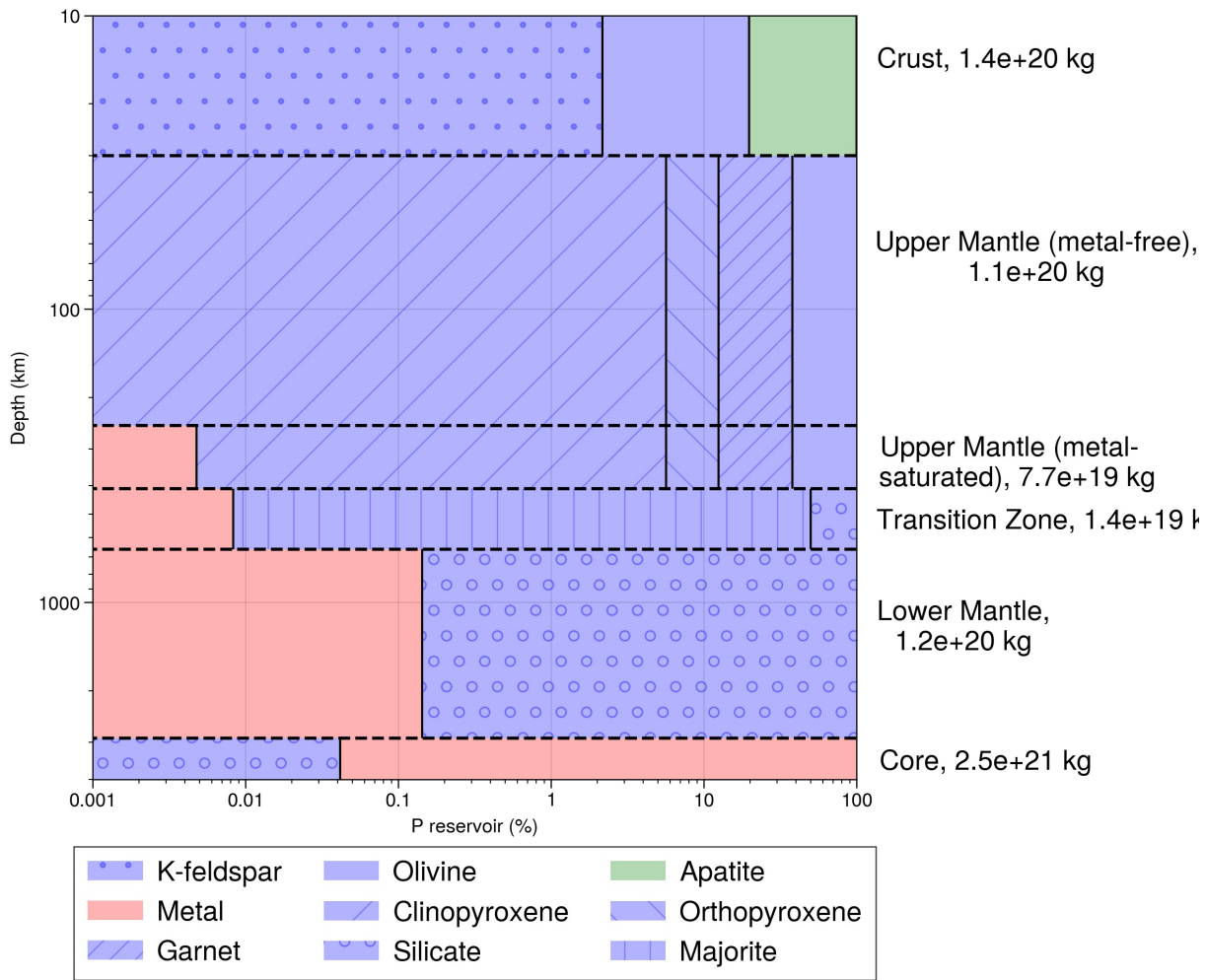


Figure 3: Phosphorus reservoir sizes and mineral-host speciation with depth in Earth, plotted as percentages of all P in a given reservoir. The fraction of siderophile reduced P hosted by metal increases from the onset of native iron metal saturation, at around 250 km depth.

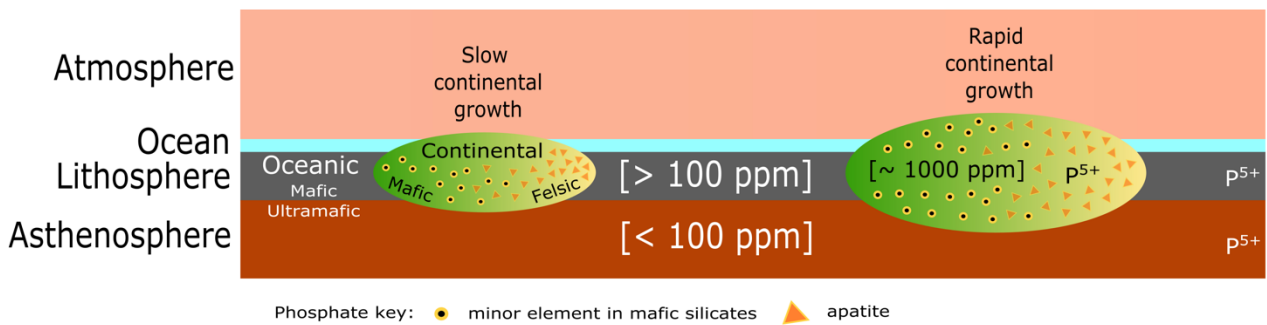


Figure 4: Uncertainties in crustal mode and P-mineralogy during the Prebiotic Era.

Continental mass may be much lower than or equal to that observed in the modern. The composition of that continental material may be mafic (broadly apatite undersaturated) or felsic (apatite saturated). Not to scale. Olivine dominates crustal P-reservoir in scenarios with slowly growing and/or mafic continental crust, whereas apatite dominates in rapidly growing and/or felsic continental crust.

Table 2: Phosphorus mineralogy of potential prebiotic relevance

Mineral name	Formulae	Paragenesis	Formation conditions and Lithologies	Geodynamic associations
Pyrophosphite	$K_2CaP_2O_7$	An	Fire	/
Pyrocoprite	$(Mg(K,Na))_2P_2O_7$	An	Fire	/
Arnhemite	$(K,Na)_2Mg_2(P_2O_7) \cdot 5(H_2O)$	An	Fire	/
Hylbrownite	$Na_3MgP_3O_{10} \cdot 12H_2O$	LTS (S)	Polymetallic sulphide-ox	/
Wooldridgeite	$Na_2CaCu^{2+}_2(P_2O_7)_2 \cdot 10H_2O$	LTS (S)	Sediments + ore + ox	/
Gengenbachite	$KFe_3(H_2PO_4)_2(HPO_4)_4 \cdot 6H_2O$	LTS (An)	Slag dumps	/
Haigerachite	$KFe^{3+}_3(H_2PO_4)_6(HPO_4)_2 \cdot 4H_2O$	LTS (S)	As-Pb-ox	/
Struvite-(K)	$KMg(PO_4) \cdot 6H_2O$	LTS (S/LH)	Dolostone, Pb-ox	/
Ludjibaite	$Cu_5(PO_4)_2(OH)_4$	LTS (S)	Cu-ox	/
Cornetite	$Cu_3(PO_4)(OH)_3$	LTS (S)	Cu-ox	/
Reichenbachite	$Cu_5(PO_4)_2(OH)_4$	LTS (S)	Cu-ox	/
Hureaulite	$Mn^{2+}_5(PO_3OH)_2(PO_4)_2 \cdot 4H_2O$	HTS/LTS (S/LH)	Granite pegmatite + ox	/
Libethenite	$Cu_2(PO_4)(OH)$	LTS (S)	Cu-ox	/
Pseudomalachite	$Cu_5(PO_4)_2(OH)_4$	LTS	Cu-ox	/
Turquoise	$CuAl_6(PO_4)_4(OH)_8 \cdot 4H_2O$	HTS/LTS (S)	Cu-ox	/
Kanonerovite	$Na_3MnP_3O_{10} \cdot 12H_2O$	LTS (S/LH)	Granite pegmatite + ox	B1 / B2
Pyromorphite	$Pb_5(PO_4)_3Cl$	LTS/Volcanic Sublimate	Pb-ox	/
Negevite	NiP_2	HTS	Ultra-reducing high-T metamorphism	/
Zuktamrurite	FeP_2	HTS	Ultra-reducing high-T metamorphism	/
Murashkoite	FeP	HTS	Ultra-reducing high-T metamorphism	/
Halamishite	Ni_5P_4	HTS	Ultra-reducing high-T metamorphism	/
Transjordanite	Ni_2P	HTS	Ultra-reducing high-T metamorphism	/
Cyclophosphate(s)	e.g., $(Ni,Fe)_2P_4O_{12}$	HTS	Ultra-reducing high-T metamorphism	/
Canaphite	$Na_2CaP_2O_7 \cdot 4H_2O$	LTS (S/LH/A)	Lake sediments	/
Variscite	$Al(PO_4) \cdot 2H_2O$	LTS (S/LH/)	Sedimentary/volcanic rocks, UAFW chemistry (AS)	/
Brushite	$Ca(PO_3OH) \cdot 2H_2O$	LTS (A)	Clay-water interface, UAFW chemistry (AS)	/
Biphosphammite	$(NH_4,K)H_2(PO_4)$	LTS	Phosphate-rich rocks (AU)	/
Archerite	$H_2K(PO_4)$	LTS	Stalacites and wall rocks of caves	/
Phosphammite	$(NH_4)_2(PO_3OH)$	LTS	UAFW chemistry (AS)	/
Mundrabillaite	$(NH_4)_2Ca(PO_3OH)_2 \cdot H_2O$	LTS	UAFW chemistry (AS)	/
Swaknoite	$(NH_4)_2Ca(PO_3OH)_2 \cdot H_2O$	LTS	UAFW chemistry (AS)	/
Dittmarite	$(NH_4)Mg(PO_4) \cdot H_2O$	LTS	UAFW chemistry (AS)	/
Stercorite	$(NH_4)Na(PO_3OH) \cdot 4H_2O$	LTS	UAFW chemistry (AS)	/

Bobierrite	$Mg_3(PO_4)_2 \cdot 8H_2O$	LTS	UAFW chemistry (AS)	/
Schertelite	$(NH_4)_2Mg(PO_3OH)_2 \cdot 4H_2O$	LTS	UAFW chemistry (AS)	/
Hannayite	$(NH_4)_2Mg_3(PO_3OH)_4 \cdot 8H_2O$	LTS	UAFW chemistry (AS)	/
Niahite	$(NH_4)Mn^{2+}(PO_4) \cdot H_2O$	LTS	Phosphate-rich rocks	/
Lüneburgite	$Mg_3[B_2(OH)_6(PO_4)_2] \cdot 6H_2O$	LTS (A)	Evaporites + dolomitic marls (SD), UAFW chemistry (AS)	/
Childrenite	$Fe^{2+}Al(PO_4)(OH)_2 \cdot H_2O$	LTS	Granite pegmatites (GR)	B1 / B2
Wagnerite	$Mg_2(PO_4)F$	Primary/HTS	Granite pegmatites (GR), metamorphic	B1 / B2
Hydroxylapatite	$Ca_5(PO_4)_3OH$	HTS/LTS	Granite pegmatite (GR), serpentinite (SP)	A / B1 / B2
Triplite	$(Mn_{2+}, Fe_{2+})_2(PO_4)F$	Primary/HTS	Granite pegmatites (GR)	B1 / B2
Hydroxylherderite	$CaBe(PO_4)(OH)$	Primary/HTS	Be-Granite pegmatite (GR)	B1 / B2
Whitlockite	$Ca_9Mg(PO_3OH)(PO_4)_6$	HTS/LTS (S/LH)	Granite pegmatites (GR), P-rich rocks	B1 / B2
Monetite	$Ca(PO_3OH)$	LTS (S/LH)	Granite pegmatite + ox, UAFW chemistry	B1 / B2
Nahpoite	$Na_2(PO_3OH)$	LTS (S/LH/A)	Phosphatic Ironstone; alkaline magmatism (AK)	B1 / B2
Herderite	$CaBe(PO_4)F$	LTS (S/LH)	Be-Granite pegmatite (GR)	B1 / B2
Schreibersite	$(Fe, Ni)_3P$	Primary	Reduced igneous rocks, impact-craters/sediments (VP)	A / B1 / B2
Monazite-(La)	$La(PO_4)$	Primary/HTS	Granite and gneiss (GR)	B1 / B2
Dorfmanite	$Na_2(PO_3OH) \cdot 2H_2O$	HTS/LTS	Alkaline magmatism (AK)	B1 / B2
Xenotime-(Y)	$Y(PO_4)$	Primary/HTS	AK, granites, gneiss, alpine veins (GR)	A / B1 / B2
Monazite-(Ce)	$Ce(PO_4)$	Primary/HTS/LTS (A)	Common igneous phase (GR)	A / B1 / B2
Vivianite	$Fe^{2+}_3(PO_4)_2 \cdot 8H_2O$	Primary/HTS/LTS (S/LH/A)	Granite pegmatite (GR-P?), authigenic marine (AU)	A / B1 / B2
Chlorapatite	$Ca_5(PO_4)_3Cl$	Primary/HTS/LTS	Igneous, metamorphic (GR, MA)	A / B1 / B2
Wavellite	$Al_3(PO_4)_2(OH)_3 \cdot 5H_2O$	LTS	Metamorphic, hydrothermal veins	A / B1 / B2
Newberyite	$Mg(PO_3OH) \cdot 3H_2O$	LTS	UAFW chemistry (AS)	/
Struvite	$(NH_4)Mg(PO_4) \cdot 6H_2O$	LTS	UAFW chemistry (AS)	/
Calcite	$CaCO_3$	HTS/LTS	Various	/
Iron (oxyhydr)oxides	$(CO_3^{2-})_3: [Fe^{2+}_4Fe^{3+}_2(HO^-)_{12}]^{2+} \cdot [CO_3^{2-}_3 \cdot 2H_2O]^{2-}$	HTS/LTS	Various	/
Fluorapatite	$Ca_5(PO_4)_3F$	Primary/HTS/LTS (A)	Common igneous phase (GR, MA)	A / B1 / B2
Feldspar	$KAlSi_3O_8 - NaAlSi_3O_8 - CaAl_2Si_2O_8$	Primary/HTS	Common igneous phase (GR, MA)	A / B1 / B2
Garnet	$X_3Y_2(SiO_4)_3$ (Fe, Mg, Mn, Ca; Al, Cr, Fe)	Primary/HTS	Common igneous phase (GR, MA, UM)	A / B1 / B2
Olivine	$(Mg, Fe)_2SiO_4$	Primary	Common igneous phase (MA, UM)	A / B1 / B2
Pyroxene	$MgFe(SiAl)_2O_6$	Primary/HTS	Common igneous phase (MA, UM)	A / B1 / B2
Volcanic glass	/	Primary	Common igneous phase (GR, MA, UM)	A / B1 / B2

Color codes: Unlikely. Uncertain. Possible (rare). Possible (unreactive). Likely. **General paragenetic codes:** (A) – anthropogenic; HTS – high temperature secondary; LTS – low temperature secondary; LH – late hydrothermal; -ox – oxidative weathering; S – supergene. **Setting-specific paragenetic codes:** AS – alternative solvent. AK –

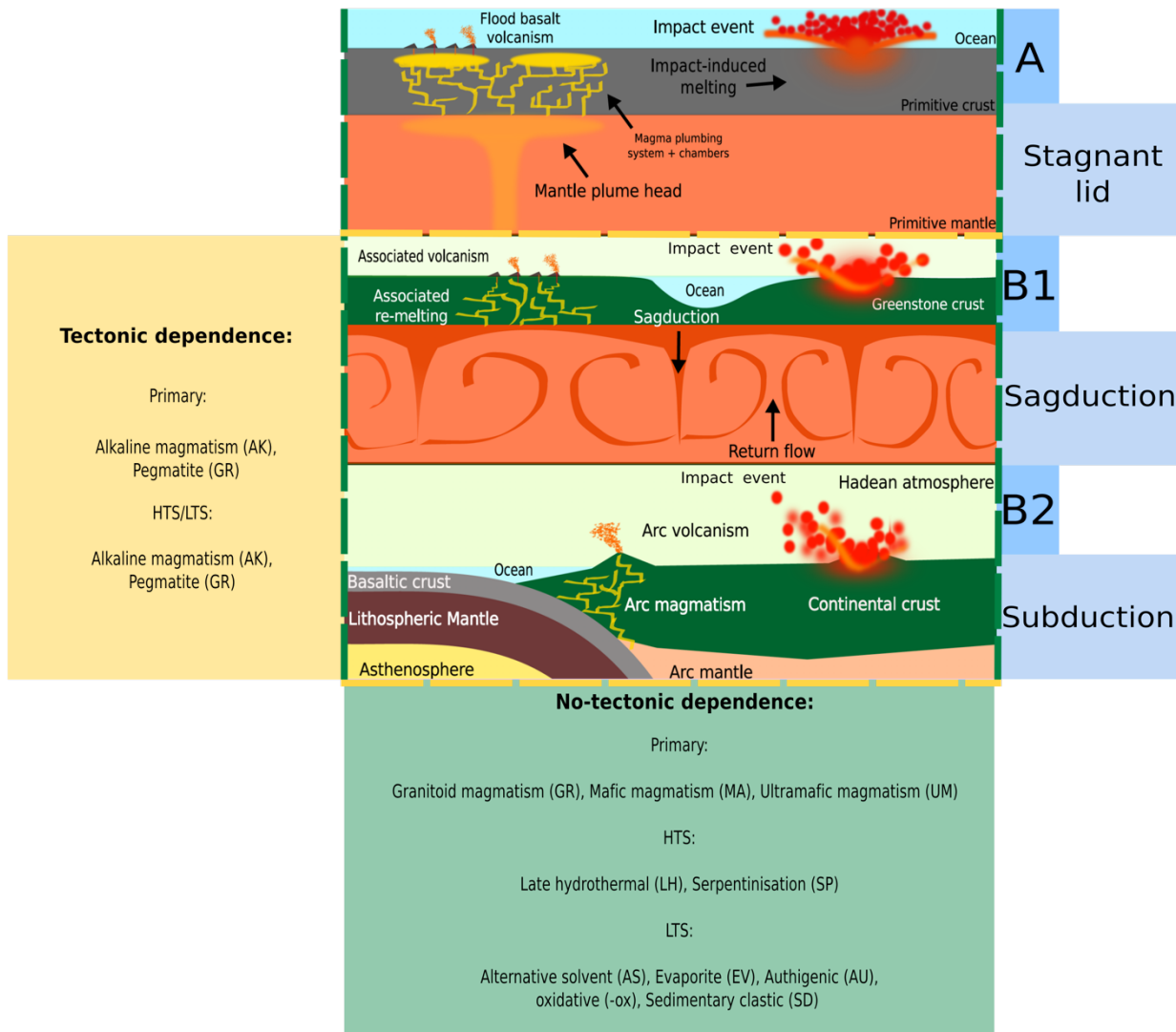


Figure 5: Possible geological processes and mineralization settings in the Hadean Eon. Not to scale, but “sagduction” crust > Hadean crust > 3 Ga oceanic basaltic crust. The paragenetic modes associated with either all three or only regimes B1/B2 are indicated. HTS = high temperature secondary; LTS = low temperature secondary.

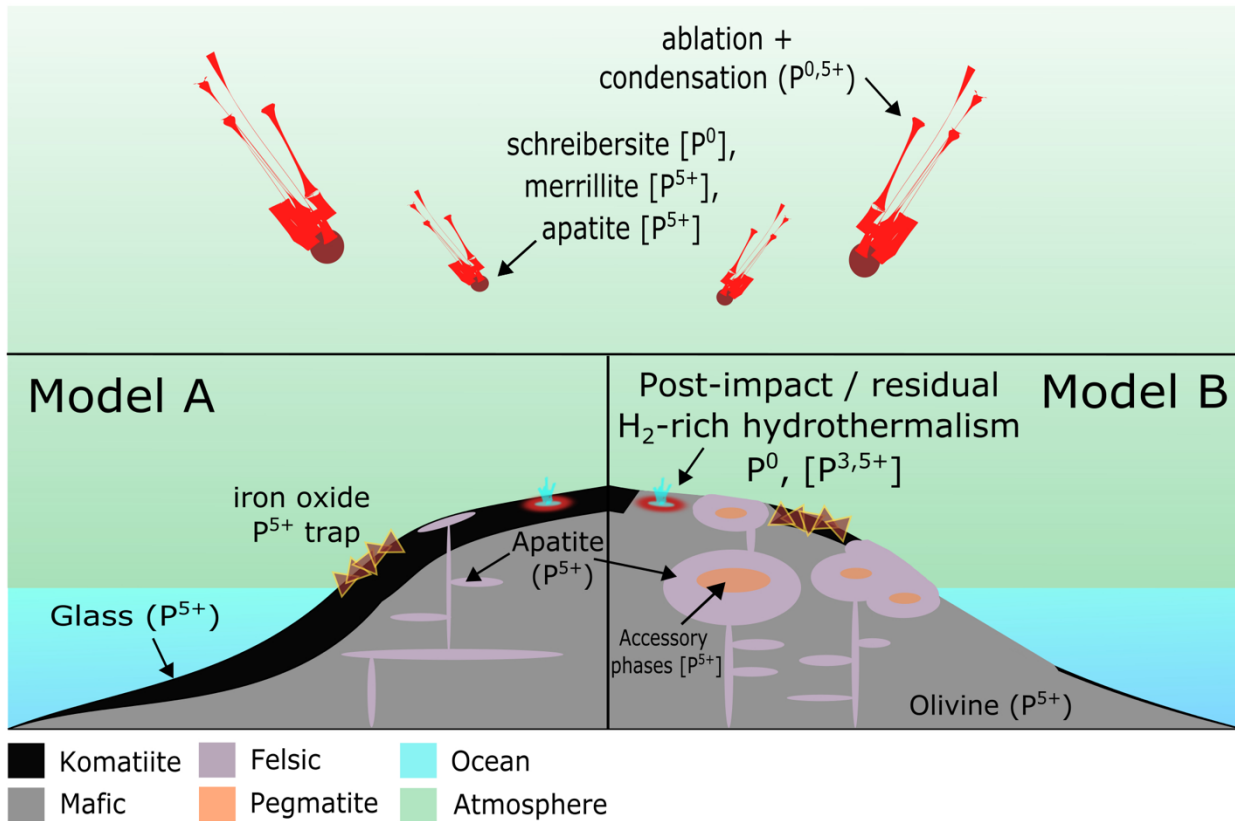


Figure 6: Prebiotically relevant phosphorus-bearing phases on early Earth. The relative abundance of prebiotically important endogenous phases is principally dependent on crustal composition (more komatiite in Model A, less in Model B; less versus more granitoids and basalt). The abundance of meteoritic schreibersite is independent of these uncertainties. Major oxidation states of P in each source are indicated.

Table 3: Challenges and advantages of specific phases as P sources in prebiotic chemistry

Phase	Challenges / advantages	Ideal conditions for P release
Exogenous		
<i>Schreibersite</i>	Stochastic delivery; short window of post-deposition availability / highly soluble and reactive towards organics, common in meteorites	P-rich iron impactor directly depositing into low-volume target environment / ultra-reducing terrestrial environments
<i>Alternative phosphides</i>	Paragenesis appears to require biological intervention / highly soluble and reactive towards organics	P-rich impactor directly depositing into low-volume target environment / ultra-reducing terrestrial environments
<i>Apatite/merrillite</i>	Stochastic delivery; moderate post-deposition window of availability; poor solubility (depending on local conditions) / common in meteorites	P-rich impactor directly depositing into low-volume target environment
<i>Vapor condensates</i>	Stochastic delivery; very short post-deposition window of availability / high surface area; potentially highly soluble depending on redox state and chemical formula	Large P-rich impactor vaporising in vicinity of target environment
Endogenous		
<i>Schreibersite</i>	Very rare, if possible at all / linked to reducing conditions useful for other prebiotic chemistry	Massive P-rich iron impact generating H ₂ -rich magmas
<i>Apatite</i>	Poor solubility under many conditions; potentially globally rare, depending on crustal regime / highly soluble under some specific circumstances; potentially globally abundant, depending on crustal regime	Raid early growth of felsic apatite-rich continental crust
<i>Alternative phosphates</i>	Very rare, if possible at all; generally very low solubility	Raid early growth of felsic apatite-rich continental crust; active tectonics
<i>Mafic silicates</i>	Low P-concentrations; P mobility governed by local iron-redox chemistry during weathering / potentially globally abundant, depending on crustal regime	Anoxic weathering regime; slow growth of felsic apatite-rich continental crust; no active tectonics

References

- Bali, E., Audétat, A., Keppler, H., 2013. Water and hydrogen are immiscible in Earth's mantle. *Nature* 495, 220. <https://doi.org/10.1038/nature11908>
- Barge, L.M., Cardoso, S.S.S., Cartwright, J.H.E., Cooper, G.J.T., Cronin, L., Wit, A.D., Doloboff, I.J., Escribano, B., Goldstein, R.E., Haudin, F., Jones, D.E.H., Mackay, A.L., Maselko, J., Pagano, J.J., Pantaleone, J., Russell, M.J., Sainz-Díaz, C.I., Steinbock, O., Stone, D.A., Tanimoto, Y., Thomas, N.L., 2015. From Chemical Gardens to Chemobionics. *Chem Rev* 115, 8652–8703. <https://doi.org/10.1021/acs.chemrev.5b00014>
- Benner, S.A., Bell, E.A., Biondi, E., Brassler, R., Carell, T., Kim, H., Mojzsis, S.J., Omran, A., Pasek, M.A., Trail, D., 2020. When Did Life Likely Emerge on Earth in an RNA-First Process? *Chemsystemschem* 2. <https://doi.org/10.1002/syst.201900035>
- Binzel, R.P., Xu, S., Bus, S.J., Skrutskie, M.F., Meyer, M.R., Knezek, P., Barker, E.S., 1993. Discovery of a Main-Belt Asteroid Resembling Ordinary Chondrite Meteorites. *Science* 262, 1541–1543. <https://doi.org/10.1126/science.262.5139.1541>
- Bowler, M.W., Cliff, M.J., Waltho, J.P., Blackburn, G.M., 2010. Why did Nature select phosphate for its dominant roles in biology? *New J Chem* 34, 784–794. <https://doi.org/10.1039/b9nj00718k>
- Brantley, S.L., Olsen, A.A., 2014. *Treatise on Geochemistry* 69–113. <https://doi.org/10.1016/b978-0-08-095975-7.00503-9>
- Brett, R., Sato, M., 1984. Intrinsic oxygen fugacity measurements on seven chondrites, a pallasite, and a tektite and the redox state of meteorite parent bodies. *Geochim Cosmochim Acta* 48, 111–120. [https://doi.org/10.1016/0016-7037\(84\)90353-3](https://doi.org/10.1016/0016-7037(84)90353-3)
- Britvin, S.N., Murashko, M.N., Vapnik, Y., Polekhovskiy, Y.S., Krivovichev, S.V., 2015. Earth's Phosphides in Levant and insights into the source of Archean prebiotic phosphorus. *Sci Rep* 5, 8355. <https://doi.org/10.1038/srep08355>
- Britvin, S.N., Murashko, M.N., Vapnik, Y., Vlasenko, N.S., Krzhizhanovskaya, M.G., Vereshchagin, O.S., Bocharov, V.N., Lozhkin, M.S., 2020. Cyclophosphates, a new class of native phosphorus compounds, and some insights into prebiotic phosphorylation on early Earth. *Geology* 49. <https://doi.org/10.1130/g48203.1>
- Broska, I., Petrik, I., 2008. Genesis and stability of accessory phosphates in silicic magmatic rocks: a Western Carpathian case study. *Mineralogia* 39, 53–66. <https://doi.org/10.2478/v10002-008-0004-6>
- Brownlee, D., Joswiak, D., Matrajt, G., 2012. Overview of the rocky component of Wild 2 comet samples: Insight into the early solar system, relationship with meteoritic materials and the differences between comets and asteroids. *Meteorit Planet Sci* 47, 453–470. <https://doi.org/10.1111/j.1945-5100.2012.01339.x>

- Brunet, F., Chazot, G., 2001. Partitioning of phosphorus between olivine, clinopyroxene and silicate glass in a spinel lherzolite xenolith from Yemen. *Chem Geol* 176, 51–72. [https://doi.org/10.1016/s0009-2541\(00\)00351-x](https://doi.org/10.1016/s0009-2541(00)00351-x)
- Bryant, D.E., Greenfield, D., Walshaw, R.D., Johnson, B.R.G., Herschy, B., Smith, C., Pasek, M.A., Telford, R., Scowen, I., Munshi, T., Edwards, H.G.M., Cousins, C.R., Crawford, I.A., Kee, T.P., 2013. Hydrothermal modification of the Sikhote-Alin iron meteorite under low pH geothermal environments. A plausibly prebiotic route to activated phosphorus on the early Earth. *Geochim Cosmochim Acta* 109, 90–112. <https://doi.org/10.1016/j.gca.2012.12.043>
- Burcar, B., Pasek, M., Gull, M., Cafferty, B.J., Velasco, F., Hud, N.V., Menor-Salván, C., 2016. Darwin's Warm Little Pond: A One-Pot Reaction for Prebiotic Phosphorylation and the Mobilization of Phosphate from Minerals in a Urea-Based Solvent. *Angewandte Chemie Int Ed* 55, 13249–13253. <https://doi.org/10.1002/anie.201606239>
- Buseck, P.R., 1977. Pallasite meteorites—mineralogy, petrology and geochemistry. *Geochim Cosmochim Acta* 41, 711–740. [https://doi.org/10.1016/0016-7037\(77\)90044-8](https://doi.org/10.1016/0016-7037(77)90044-8)
- Chaïrat, C., Schott, J., Oelkers, E.H., Lartigue, J.-E., Harouiya, N., 2007. Kinetics and mechanism of natural fluorapatite dissolution at 25°C and pH from 3 to 12. *Geochim Cosmochim Acta* 71, 5901–5912. <https://doi.org/10.1016/j.gca.2007.08.031>
- Costanzo, G., Saladino, R., Crestini, C., Ciciriello, F., Mauro, E.D., 2007. Nucleoside Phosphorylation by Phosphate Minerals. *J Biol Chem* 282, 16729–16735. <https://doi.org/10.1074/jbc.m611346200>
- Cox, G.M., Lyons, T.W., Mitchell, R.N., Hasterok, D., Gard, M., 2018. Linking the rise of atmospheric oxygen to growth in the continental phosphorus inventory. *Earth Planet Sc Lett* 489, 28–36. <https://doi.org/10.1016/j.epsl.2018.02.016>
- Dhuime, B., Hawkesworth, C.J., Delavault, H., Cawood, P.A., 2017. Continental growth seen through the sedimentary record. *Sediment Geol* 357, 16–32. <https://doi.org/10.1016/j.sedgeo.2017.06.001>
- Dhuime, B., Wuestefeld, A., Hawkesworth, C.J., 2015. Emergence of modern continental crust about 3 billion years ago. *Nat Geosci* 8, 552–555. <https://doi.org/10.1038/ngeo2466>
- Dodd, M.S., Papineau, D., Grenne, T., Slack, J.F., Rittner, M., Pirajno, F., O'Neil, J., Little, C.T.S., 2017. Evidence for early life in Earth's oldest hydrothermal vent precipitates. *Nature* 543, 60. <https://doi.org/10.1038/nature21377>
- Douglas, K., Mangan, T., Carrillo-Sanchez, J.D., Bones, D., Feng, W., Blitz, M., Plane, J., 2020. Meteor Ablated Phosphorus as a Source of Bioavailable P to the Terrestrial Planets. <https://doi.org/10.5194/egusphere-egu2020-10457>
- Fegley, B., Lewis, J.S., 1980. Volatile Element Chemistry in the Solar Nebula" Na, K, F, Cl, Br, and P. *Icarus* 41, 439–455.
- Fernández-García, C., Coggins, A.J., Powner, M.W., 2017. A Chemist's Perspective on the Role of Phosphorus at the Origins of Life. *Life* 7, 31. <https://doi.org/10.3390/life7030031>

- Frost, D.J., Liebske, C., Langenhorst, F., McCammon, C.A., Trønnes, R.G., Rubie, D.C., 2004. Experimental evidence for the existence of iron-rich metal in the Earth's lower mantle. *Nature* 428, 409–412. <https://doi.org/10.1038/nature02413>
- Gale, A., Dalton, C.A., Langmuir, C.H., Su, Y., Schilling, J., 2013. The mean composition of ocean ridge basalts. *Geochem Geophys Geosystems* 14, 489–518. <https://doi.org/10.1029/2012gc004334>
- Graaf, de, Visscher, J., Schwartz, A.W., 1995. A plausibly prebiotic synthesis of phosphonic acids. *Nature* 378.
- Greber, N.D., Dauphas, N., 2019. The chemistry of fine-grained terrigenous sediments reveals a chemically evolved Paleoproterozoic emerged crust. *Geochim Cosmochim Acta*. <https://doi.org/10.1016/j.gca.2019.04.012>
- Greber, N.D., Dauphas, N., Bekker, A., Ptáček, M.P., Bindeman, I.N., Hofmann, A., 2017. Titanium isotopic evidence for felsic crust and plate tectonics 3.5 billion years ago. *Science* 357, 1271–1274. <https://doi.org/10.1126/science.aan8086>
- Green, T.H., Watson, E.B., 1982. Crystallization of apatite in natural magmas under high pressure, hydrous conditions, with particular reference to 'Orogenic' rock series. *Contrib Mineral Petr* 79, 96–105. <https://doi.org/10.1007/bf00376966>
- Grosch, E.G., Hazen, R.M., 2015. Microbes, Mineral Evolution, and the Rise of Microcontinents—Origin and Coevolution of Life with Early Earth. *Astrobiology* 15, 922–939. <https://doi.org/10.1089/ast.2015.1302>
- Haggerty, S.E., Fung, A.T., Burt, D.M., 1994. Apatite, phosphorus and titanium in eclogitic garnet from the upper mantle. *Geophys Res Lett* 21, 1699–1702. <https://doi.org/10.1029/94gl01001>
- Harouiya, N., Chaïrat, C., Köhler, S.J., Gout, R., Oelkers, E.H., 2007. The dissolution kinetics and apparent solubility of natural apatite in closed reactors at temperatures from 5 to 50 °C and pH from 1 to 6. *Chem Geol* 244, 554–568. <https://doi.org/10.1016/j.chemgeo.2007.07.011>
- Hart, R.J., Andreoli, M.A.G., Smith, C.B., Otter, M.L., Durrheim, R., 1990. Ultramafic rocks in the centre of the Vredefort structure (South Africa): Possible exposure of the upper mantle? *Chem Geol* 83, 233–248. [https://doi.org/10.1016/0009-2541\(90\)90282-c](https://doi.org/10.1016/0009-2541(90)90282-c)
- Hawkesworth, C., Jaupart, C., 2021. Heat flow constraints on the mafic character of Archean continental crust. *Earth Planet Sc Lett* 571, 117091. <https://doi.org/10.1016/j.epsl.2021.117091>
- Hazen, R.M., 2013. Paleomineralogy of the Hadean Eon: A preliminary species list. *Am J Sci* 313, 807–843. <https://doi.org/10.2475/09.2013.01>
- Hazen, R.M., Papineau, D., Bleeker, W., Downs, R.T., Ferry, J.M., McCoy, T.J., Sverjensky, D.A., Yang, H., 2008. Review Paper. Mineral evolution. *Am Mineral* 93, 1693–1720. <https://doi.org/10.2138/am.2008.2955>

- Herschy, B., Chang, S.J., Blake, R., Lepland, A., Abbott-Lyon, H., Sampson, J., Atlas, Z., Kee, T.P., Pasek, M.A., 2018. Archean phosphorus liberation induced by iron redox geochemistry. *Nat Commun* 9, 1346. <https://doi.org/10.1038/s41467-018-03835-3>
- Holm, N.G., 2014. Glasses as sources of condensed phosphates on the early earth. *Geochem T* 15, 8. <https://doi.org/10.1186/1467-4866-15-8>
- Huang, Y., Chubakov, V., Mantovani, F., Rudnick, R.L., McDonough, W.F., 2013. A reference Earth model for the heat-producing elements and associated geoneutrino flux. *Geochem Geophys Geosystems* 14, 2003–2029. <https://doi.org/10.1002/ggge.20129>
- Hystad, G., Eleish, A., Hazen, R.M., Morrison, S.M., Downs, R.T., 2019. Bayesian Estimation of Earth's Undiscovered Mineralogical Diversity Using Noninformative Priors. *Math Geosci* 51, 401–417. <https://doi.org/10.1007/s11004-019-09795-8>
- Islam, S., Powner, M.W., 2017. Prebiotic Systems Chemistry: Complexity Overcoming Clutter. *Chem* 2, 470–501. <https://doi.org/10.1016/j.chempr.2017.03.001>
- Jahnke, R.A., 1992. 14 The Phosphorus Cycle. *Int Geophys* 50, 301–315. [https://doi.org/10.1016/s0074-6142\(08\)62697-2](https://doi.org/10.1016/s0074-6142(08)62697-2)
- Jahnke, R.A., 1984. The synthesis and stability of carbonate fluorapatite. *American Journal of Science* 284, 58–78.
- Jenner, F.E., Bennett, V.C., Yaxley, G., Friend, C.R.L., Nebel, O., 2013. Eoarchean within-plate basalts from southwest Greenland. *Geology* 41, 327–330. <https://doi.org/10.1130/g33787.1>
- Johnson, T.E., Brown, M., Gardiner, N.J., Kirkland, C.L., Smithies, R.H., 2017. Earth's first stable continents did not form by subduction. *Nature* 543, 239. <https://doi.org/10.1038/nature21383>
- Takegawa, T., Noda, M., Nannri, H., 2002. Geochemical Cycles of Bio-essential Elements on the Early Earth and Their Relationships to Origin of Life. *Resour Geol* 52, 83–89. <https://doi.org/10.1111/j.1751-3928.2002.tb00121.x>
- Kamerlin, S.C.L., Sharma, P.K., Prasad, R.B., Warshel, A., 2013. Why nature really chose phosphate. *Q Rev Biophys* 46, 1–132. <https://doi.org/10.1017/s0033583512000157>
- Kaminsky, F., 2012. Mineralogy of the lower mantle: A review of 'super-deep' mineral inclusions in diamond. *Earth-sci Rev* 110, 127–147. <https://doi.org/10.1016/j.earscirev.2011.10.005>
- Kee, T.P., Bryant, D.E., Herschy, B., Marriott, K.E.R., Cosgrove, N.E., Pasek, M.A., Atlas, Z.D., Cousins, C.R., 2013. Phosphate Activation via Reduced Oxidation State Phosphorus (P). Mild Routes to Condensed-P Energy Currency Molecules. *Life* 3, 386–402. <https://doi.org/10.3390/life3030386>
- Keller, C.B., Schoene, B., 2012. Statistical geochemistry reveals disruption in secular lithospheric evolution about 2.5 Gyr ago. *Nature* 485, 490. <https://doi.org/10.1038/nature11024>

- Korenaga, J., 2018. Estimating the formation age distribution of continental crust by unmixing zircon ages. *Earth Planet Sc Lett* 482, 388–395. <https://doi.org/10.1016/j.epsl.2017.11.039>
- Lebouteiller, V., Kuassivi, Ferlet, R., 2005. Phosphorus in the Diffuse Interstellar Medium. <https://doi.org/10.1051/0004-6361:20053448>
- Lipp, A.G., Shorttle, O., Syvret, F., Roberts, G.G., 2020. Major Element Composition of Sediments in Terms of Weathering and Provenance: Implications for Crustal Recycling. *Geochem Geophys Geosystems* 21. <https://doi.org/10.1029/2019gc008758>
- Liu, Z., Rossi, J.-C., Pascal, R., 2019. How Prebiotic Chemistry and Early Life Chose Phosphate. *Life* 9, 26. <https://doi.org/10.3390/life9010026>
- Lodders, K., 2003. SOLAR SYSTEM ABUNDANCES AND CONDENSATION TEMPERATURES OF THE ELEMENTS. *The Astrophysical Journal* 591, 1220–1247.
- London, D., 2018. Ore-Forming Processes Within Granitic Pegmatites. *Ore Geol Rev* 101, 349–383. <https://doi.org/10.1016/j.oregeorev.2018.04.020>
- Mallmann, G., O'Neill, H.St.C., 2009. The Crystal/Melt Partitioning of V during Mantle Melting as a Function of Oxygen Fugacity Compared with some other Elements (Al, P, Ca, Sc, Ti, Cr, Fe, Ga, Y, Zr and Nb). *J Petrol* 50, 1765–1794. <https://doi.org/10.1093/petrology/egp053>
- Marchi, S., Bottke, W.F., Elkins-Tanton, L.T., Bierhaus, M., Wuennemann, K., Morbidelli, A., Kring, D.A., 2014. Widespread mixing and burial of Earth's Hadean crust by asteroid impacts. *Nature* 511, 578. <https://doi.org/10.1038/nature13539>
- McCoy-West, A.J., Chowdhury, P., Burton, K.W., Sossi, P., Nowell, G.M., Fitton, J.G., Kerr, A.C., Cawood, P.A., Williams, H.M., 2019. Extensive crustal extraction in Earth's early history inferred from molybdenum isotopes. *Nat Geosci* 12, 946–951. <https://doi.org/10.1038/s41561-019-0451-2>
- McDonough, W.F., Sun, S. -s., 1995. The composition of the Earth. *Chem Geol* 120, 223–253. [https://doi.org/10.1016/0009-2541\(94\)00140-4](https://doi.org/10.1016/0009-2541(94)00140-4)
- McSween, H.Y., Labotka, T.C., 1993. Oxidation during metamorphism of the ordinary chondrites. *Geochimica et Cosmochemica Acta* 57, 1105–1114.
- Mehta, C., Perez, A., Thompson, G., Pasek, M.A., 2018. Caveats to Exogenous Organic Delivery from Ablation, Dilution, and Thermal Degradation. *Life* 8, 13. <https://doi.org/10.3390/life8020013>
- Mininni, C., Fontani, F., Rivilla, V.M., Beltrán, M.T., Caselli, P., Vasyunin, A., 2018. On the origin of phosphorus nitride in star-forming regions. *Mon Notices Royal Astronomical Soc Lett* 476, L39–L44. <https://doi.org/10.1093/mnrasl/sly026>
- Morrison, S.M., Runyon, S.E., Hazen, R.M., 2018. The Paleomineralogy of the Hadean Eon Revisited. *Life* 8, 64. <https://doi.org/10.3390/life8040064>

- O'Neill, H.S.C., Jenner, F.E., 2012. The global pattern of trace-element distributions in ocean floor basalts. *Nature* 491, 698. <https://doi.org/10.1038/nature11678>
- Palme, H., O'Neill, H.S.C., 2014. Cosmochemical Estimates of Mantle Composition. *Treatise on Geochemistry* 2nd Edition. <https://doi.org/10.1016/b978-0-08-095975-7.00201-1>
- Pan, H., Darvell, B.W., 2010. Effect of Carbonate on Hydroxyapatite Solubility. *Cryst Growth Des* 10, 845–850. <https://doi.org/10.1021/cg901199h>
- Pan, H.-B., Darvell, B.W., 2009. Calcium Phosphate Solubility: The Need for Re-Evaluation. *Cryst Growth Des* 9, 639–645. <https://doi.org/10.1021/cg801118v>
- Pasek, M.A., 2019a. Phosphorus volatility in the early Solar nebula. *Icarus* 317, 59–65. <https://doi.org/10.1016/j.icarus.2018.07.011>
- Pasek, M.A., 2019b. A role for phosphorus redox in emerging and modern biochemistry. *Curr Opin Chem Biol* 49, 53–58. <https://doi.org/10.1016/j.cbpa.2018.09.018>
- Pasek, M.A., 2017. Schreibersite on the early Earth: Scenarios for prebiotic phosphorylation. *Geosci Front* 8, 329–335. <https://doi.org/10.1016/j.gsf.2016.06.008>
- Pasek, M.A., Dworkin, J.P., Lauretta, D.S., 2007. A radical pathway for organic phosphorylation during schreibersite corrosion with implications for the origin of life. *Geochim Cosmochim Acta* 71, 1721–1736. <https://doi.org/10.1016/j.gca.2006.12.018>
- Pasek, M.A., Gull, M., Herschy, B., 2017. Phosphorylation on the early earth. *Chem Geol.* <https://doi.org/10.1016/j.chemgeo.2017.11.008>
- Pasek, M.A., Harnmeijer, J.P., Buick, R., Gull, M., Atlas, Z., 2013. Evidence for reactive reduced phosphorus species in the early Archean ocean. *Proc National Acad Sci* 110, 10089–10094. <https://doi.org/10.1073/pnas.1303904110>
- Pasek, M.A., Herschy, B., Kee, T.P., 2015. Phosphorus: a Case for Mineral-Organic Reactions in Prebiotic Chemistry. *Origins Life Evol B* 45, 207–218. <https://doi.org/10.1007/s11084-015-9420-y>
- Pasek, M.A., Lauretta, D., 2008. Extraterrestrial Flux of Potentially Prebiotic C, N, and P to the Early Earth. *Origins Life Evol B* 38, 5–21. <https://doi.org/10.1007/s11084-007-9110-5>
- Patel, B.H., Percivalle, C., Ritson, D.J., Duffy, C.D., Sutherland, J.D., 2015. Common origins of RNA, protein and lipid precursors in a cyanosulfidic protometabolism. *Nat Chem* 7, 301–307. <https://doi.org/10.1038/nchem.2202>
- Paytan, A., McLaughlin, K., 2007. The Oceanic Phosphorus Cycle. *Chem Rev* 107, 563–576. <https://doi.org/10.1021/cr0503613>
- Pearce, E.I.F., 1988. On the Dissolution of Hydroxyapatite in Acid Solutions. *J Dent Res* 67, 1056–1058. <https://doi.org/10.1177/00220345880670070801>

- Piani, L., Marrocchi, Y., Rigaudier, T., Vacher, L.G., Thomassin, D., Marty, B., 2020. Earth's water may have been inherited from material similar to enstatite chondrite meteorites. *Sci New York N Y* 369, 1110–1113. <https://doi.org/10.1126/science.aba1948>
- Pirim, C., Pasek, M.A., Sokolov, D.A., Sidorov, A.N., Gann, R.D., Orlando, T.M., 2014. Investigation of schreibersite and intrinsic oxidation products from Sikhote-Alin, Seymchan, and Odessa meteorites and Fe₃P and Fe₂NiP synthetic surrogates. *Geochim Cosmochim Acta* 140, 259–274. <https://doi.org/10.1016/j.gca.2014.05.027>
- Prigiobbe, V., Costa, G., Baciocchi, R., Hänchen, M., Mazzotti, M., 2009. The effect of CO₂ and salinity on olivine dissolution kinetics at 120°C. *Chem Eng Sci* 64, 3510–3515. <https://doi.org/10.1016/j.ces.2009.04.035>
- Righter, K., Pando, K., Humayun, M., Waesermann, N., Yang, S., Boujibar, A., Danielson, L.R., 2018. Effect of Silicon on Activity Coefficients of Siderophile Elements (Au, Pd, Pt, P, Ga, Cu, Zn, and Pb) in Liquid Fe: Roles of Core Formation, Late Sulfide Matte, and Late Veneer in Shaping Terrestrial Mantle Geochemistry. *Geochim Cosmochim Acta*. <https://doi.org/10.1016/j.gca.2018.04.011>
- Righter, K., Pando, K.M., Danielson, L., Lee, C.-T., 2010. Partitioning of Mo, P and other siderophile elements (Cu, Ga, Sn, Ni, Co, Cr, Mn, V, and W) between metal and silicate melt as a function of temperature and silicate melt composition. *Earth Planet Sc Lett* 291, 1–9. <https://doi.org/10.1016/j.epsl.2009.12.018>
- Rimmer, P.B., Shorttle, O., 2019. Origin of Life's Building Blocks in Carbon- and Nitrogen-Rich Surface Hydrothermal Vents. *Life* 9, 12. <https://doi.org/10.3390/life9010012>
- Rosas, J.C., Korenaga, J., 2018. Rapid crustal growth and efficient crustal recycling in the early Earth: Implications for Hadean and Archean geodynamics. *Earth Planet Sc Lett* 494, 42–49. <https://doi.org/10.1016/j.epsl.2018.04.051>
- Rudnick, R.L., Gao, S., 2014. Composition of the Continental Crust. *Treatise on Geochemistry* 2nd Edition. <https://doi.org/10.1016/b978-0-08-095975-7.00301-6>
- Schönbächler, M., Carlson, R.W., Horan, M.F., Mock, T.D., Hauri, E.H., 2010. Heterogeneous Accretion and the Moderately Volatile Element Budget of Earth. *Science* 328, 884–887. <https://doi.org/10.1126/science.1186239>
- Schwartz, A.W., 2006. Phosphorus in prebiotic chemistry. *Philosophical Transactions Royal Soc B Biological Sci* 361, 1743–1749. <https://doi.org/10.1098/rstb.2006.1901>
- Sikdar, J., Rai, V.K., 2020. Si-Mg isotopes in enstatite chondrites and accretion of reduced planetary bodies. *Sci Rep-uk* 10, 1273. <https://doi.org/10.1038/s41598-020-57635-1>
- Strachan, D., 2017. Glass dissolution as a function of pH and its implications for understanding mechanisms and future experiments ScienceDirect. *Geochimica et Cosmochimica Acta* 219, 111–123. <https://doi.org/10.1016/j.gca.2017.09.008>
- Sutherland, J.D., 2015. The Origin of Life—Out of the Blue. *Angewandte Chemie Int Ed* 55, 104–121. <https://doi.org/10.1002/anie.201506585>

- Sweetapple, M.T., Collins, P.L.F., 2002. Genetic Framework for the Classification and Distribution of Archean Rare Metal Pegmatites in the North Pilbara Craton, Western Australia. *Economic Geology* 97, 873–895.
- Tang, M., Chen, K., Rudnick, R.L., 2016. Archean upper crust transition from mafic to felsic marks the onset of plate tectonics. *Science* 351, 372–375.
<https://doi.org/10.1126/science.aad5513>
- Taylor, S.R., McLennan, S.M., 1995. THE GEOCHEMICAL EVOLUTION OF THE CONTINENTAL CRUST. *Reviews of Geophysics* 33, 241–265.
- Tollari, N., Toplis, M.J., Barnes, S.-J., 2006. Predicting phosphate saturation in silicate magmas: An experimental study of the effects of melt composition and temperature. *Geochim Cosmochim Acta* 70, 1518–1536. <https://doi.org/10.1016/j.gca.2005.11.024>
- Toner, J.D., Catling, D.C., 2020. A carbonate-rich lake solution to the phosphate problem of the origin of life. *Proc National Acad Sci* 117, 883–888. <https://doi.org/10.1073/pnas.1916109117>
- Toplis, M.J., Dingwell, D.B., Libourel, G., 1994. The effect of phosphorus on the iron redox ratio, viscosity, and density of an evolved ferro-basalt. *Contrib Mineral Petr* 117, 293–304.
<https://doi.org/10.1007/bf00310870>
- Trail, D., Watson, E.B., Tailby, N.D., 2011. The oxidation state of Hadean magmas and implications for early Earth's atmosphere. *Nature* 480, 79–82.
<https://doi.org/10.1038/nature10655>
- Wang, Q., Barge, L.M., Steinbock, O., 2019. Microfluidic Production of Pyrophosphate Catalyzed by Mineral Membranes with Steep pH Gradients. *Chem European J* 25, 4732–4739.
<https://doi.org/10.1002/chem.201805950>
- Watson, E.B., 1980. Apatite and phosphorus in mantle source regions: An experimental study of apatite/melt equilibria at pressures to 25 kbar. *Earth Planet Sc Lett* 51, 322–335.
[https://doi.org/10.1016/0012-821x\(80\)90214-9](https://doi.org/10.1016/0012-821x(80)90214-9)
- Watson, E.B., Cherniak, D.J., Holycross, M.E., 2015. Diffusion of phosphorus in olivine and molten basalt. *Am Mineral* 100, 2053–2065. <https://doi.org/10.2138/am-2015-5416>
- Westheimer, F.H., 1987. Why nature chose phosphates. *Science* 235, 1173–1178.
<https://doi.org/10.1126/science.2434996>
- Williams, H.M., Wood, B.J., Wade, J., Frost, D.J., Tuff, J., 2012. Isotopic evidence for internal oxidation of the Earth's mantle during accretion. *Earth Planet Sc Lett* 321, 54–63.
<https://doi.org/10.1016/j.epsl.2011.12.030>
- Yang, X., Gaillard, F., Scaillet, B., 2014. A relatively reduced Hadean continental crust and implications for the early atmosphere and crustal rheology. *Earth Planet Sc Lett* 393, 210–219.
<https://doi.org/10.1016/j.epsl.2014.02.056>

- Zanda, B., Bourot-Denise, M., Perron, C., Hewins, R.H., 1994. Origin and Metamorphic Redistribution of Silicon, Chromium, and Phosphorus in the Metal of Chondrites. *Science* 265, 1846–1849.
- Zhang, A.-C., Li, Q.-L., Yurimoto, H., Sakamoto, N., Li, X.-H., Hu, S., Lin, Y.-T., Wang, R.-C., 2016. Young asteroidal fluid activity revealed by absolute age from apatite in carbonaceous chondrite. *Nat Commun* 7, 12844. <https://doi.org/10.1038/ncomms12844>
- Zhu, F., Li, J., Liu, J., Dong, J., Liu, Z., 2019. Metallic iron limits silicate hydration in Earth's transition zone. *Proc National Acad Sci* 116, 22526–22530. <https://doi.org/10.1073/pnas.1908716116>